FATIGUE BEHAVIOR OF TOUGHENED MATERIALS

AFOSR F49620-96-1-0164 - PARENT

AFOSR F08671-9601143 - AASERT

JOHN J. LEWANDOWSKI, PI
ROBERT M. AIKIN, JR., Co-PI

Department of Materials Science and Engineering
THE CASE SCHOOL OF ENGINEERING
Case Western Reserve University
Cleveland, Ohio 44106

FINAL TECHNICAL REPORT

COVERING THE PERIOD 5/1/96 – 12/31/99

MARCH 2000

REPORT DOCUMENTATION PAGE

AFRL-SR-BL-TR-00-

0288

1. AGENCY USE ONLY (Leave blank)	2. REPORT DATE	3. REPOR... AND DATES COVERED
	March 1, 2000	Final - 1 May 1996 - 31 December 1999

4. TITLE AND SUBTITLE

Fatigue and Fracture Behavior of Toughened Material

5. FUNDING NUMBERS

F49620-96-1-0164

6. AUTHOR(S)

Professors John Lewandowski and
Robert M. Aikin, Jr.

7. PERFORMING ORGANIZATION NAME(S) AND ADDRESS(ES)

Professor John J. Lewandowski
Department of Materials Science and Engineering
Case Western Reserve University
Cleveland, OH 44016-7204

8. PERFORMING ORGANIZATION REPORT NUMBER

9. SPONSORING/MONITORING AGENCY NAME(S) AND ADDRESS(ES)

Department of the Air Force
Air Force Office of Scientific Research
Bolling Air Force Base, DC 20332-6488

10. SPONSORING/MONITORING AGENCY REPORT NUMBER

11. SUPPLEMENTARY NOTES

The reviews, opinions and/or findings contained in this report are those of the author(s) and should not be construed as an official Department of the Air Force position, policy or decision, unless so designated elsewhere.

12a. DISTRIBUTION/AVAILABILITY STATEMENT

Approved for Public Release; Distribution Unlimited

12b. DISTRIBUTION CODE

13. ABSTRACT (Maximum 200 words)

The mechanisms controlling the fatigue and fracture behavior of materials toughened with ductile/tough phases are the focus of this work. This research is utilizing materials processed at WPAFB from the binary Nb-Si system, as well recently developed Nb-Ti-Hf-Si-Al-Cr (i.e. at GE CRD) base materials in order to determine the factors controlling the mechanical behavior under both monotonic and cyclic loading conditions. Considerable work has already demonstrated the positive effects of compositing $Nb_5 Si_3$ with Nb on the toughness of such materials, although relatively little is known regarding the cyclic fatigue behavior of the materials obtained from the binary Nb-Si systems as well as those obtained via alloying. A complementary AASERT program investigated the fracture and fatigue behavior of bulk metallic glasses produced at California Institute of Technology and Howmet, Inc.

14. SUBJECT TERMS

Silicides, Intermetallics, Composites, Fatigue, Bulk Metallic Glass, Fracture Toughness

15. NUMBER OF PAGES

16. PRICE CODE

17. SECURITY CLASSIFICATION OF REPORT	18. SECURITY CLASSIFICATION OF THIS PAGE	19. SECURITY CLASSIFICATION OF ABSTRACT	20. LIMITATION OF ABSTRACT

NSN 7540-01-280-5500

Standard Form 298 (Rev. 2-89)
Prescribed by ANSI Std. Z39-18
298-102

Table of Contents

Summary

While many advanced intermetallic systems possess desirable properties such as high temperature strength and stiffness, these systems typicaly do not exhibit adequate ductility and toughness at low temperatures. In addition, there is a need for the development of advanced processing techniques in order to provide materials in adequate quantities for subsequent use. The successful utilization of these desirable material properties also requires the development of techniques to impart higher toughness without sacrificing strength.

A variety of toughening mechanisms may be utilized to impart toughness in such systems. In brittle matrix systems, toughening may be achieved via the introduction of particles which are either brittle or ductile. In the former case, toughening may occur via crack bowing and/or deflection. The introduction of ductile particles may induce ductile phase toughening. The introduction of the ductile phases imparts some damage tolerance, the details of which have been modeled and experimentally investigated in our previous AFOSR grants. Much less work has focused on the behavior of such materials under cylcic loading conditions.

The AFOSR Program at Case Western Reserve University, AFOSR F49620-96-1-0164 and AFOSR F08671-9601143 focused on key issues in the fatigue and fracture behavior of advanced intermetallic composite systems and bulk metallic glass. Complementary work on the high rate fracture behavior and fracture toughness of Nb and some Nb alloys was also conducted. Close interaction and supply of materials from GE CRD, WPAFB, Howmet, and California Institute of Technology facilitated the work conducted.

The personnel supported over the period 5/1/9 – 12/31/99 are summarized below:

Faculty:

Professor John J. Lewandowski
Professor Robert M. Aikin, Jr.

Research Associates:

Dr. Zhonghao Liu – Partial Support
Dr. P. Lowhaphandu -Partial Support
Dr. Shulin Wen - Partial Support

Graduate Assistants:

Mr. Anand Samant	- M.S. Student	-	Full Support
Mr. P. Lowhaphandu	- Ph.D. Student	-	Full Support
Mr. Willliam Zinsser	- M.S. Candidate	-	Full Support
Mr. Sergey Solv'yev	- M.S. Candidate	-	Partial Support
Mr. Deneesh Padhi	- M.S. Candidate	-	Full Support

Undergraduate Students:

Ms. Lorie Ludrosky
Ms. Snowy Montgomery
Ms. Sally Zwonitzer

The papers published under AFOSR support for the period 5/1/96 – 12/31/99 are summarized below:

1. Rigney, J.D. and Lewandowski, J.J. (1996). "Fracture Toughness of Nb_5Si_3/Nb *In-situ* Composites: Part I: Loading Rate Effects", *Metall. Trans A.* **27A** pp. 3292-3306.

2. Samant, A. and Lewandowski J.J. (1997) "Effects of Grain Size and Alloy Content on the Cleavage Fracture Stress of Nb", *Metall. Trans. A*, **28A,** pp 389-399.

3. Lewandowski, J.J., Ward, C., Jackson, M.R., and Hunt, W.H., Jr., eds., *Layered Materials for Structural Applications*, MRS, Vol. 434, Pittsburgh, PA, (1996).

4. Lewandowski, J.J. and Rigney, J.D. (1996). "Temperature and Loading Rate Effects on Toughness of *In-situ* Niobium Silicide-Niobium Composites", in Proc. NATO ASI-Mechanical Behavior of Materials at High Temperature", C. Moura Branco and R.O. Rithchie, eds., NATO, Portugal, pp. 535-545.

5. Samant A. and Lewandowski, J.J. (1997). "Effects of Grain Size, Alloying Additions, and Test Temperature on Toughness of Nb", *Metall. Trans A*, **28A**, pp. 2297-2307.

6. Bewlay, B., Lewandowski, J.J., and Jackson M.R. (1997). "Refractory Metal-Intermetallic *In-Situ* Composites for Aircraft Engines", *JOM,* August 1997, pp. 46-48.

7. Lewandowski, J.J. and Zinsser, W. (1998). "Effects of R-ratio on Fatigue Crack Growth of Nb-Si (ss) and Nb-10Si *In-Situ* Composites", *Metall. Trans. A.*, **29A**, pp. 1749-1757.

8. Zinsser, W. and Lewandowski, J.J. (1998), "Fatigue Crack Growth in Nb-10Si Composites", *Scripta Metall*, **38**, 12, pp. 1775-1780.

9. Zinsser, W. and Lewandowski, J.J. (1999), "Effects of Changes in Grain Size and R-ratio on Fatigue Crack Growth of pre Nb and Nb-1 Wt % Zr", *Mater Sci. and Eng.*, Submitted.

10. Lowhaphandu, P. and Lewandowski, J.J. (1999), "Effects of Heat Treatment and Cu-Infiltration on the Toughness and Fatigue Crack Growth of Porous Steels", *Metall. Trans. A.*, 30A, pp. 325-334.

11. Lowhaphandu, P. and Lewandowski, J.J. (1998), "Fracture Toughness and Notch Toughness of Bulk Metallic Glass", *Scripta Metall*, **38**, 12, pp. 1811-1817.

12. Zwonitzer, S.A., Rozak, G. and Lewandowski, J.J. (1998) "Effects of Rolling Temperature and Reduction on Microstructure and Tensile Properties of Thick Plate, P/M Mo", In Mo and Mo Alloys, (A. Crowson, J.A. Shields, P.R. Subramainan and E.S. Chen, eds.) TMS-AIME, Warrendale, PA, pp. 111-124.

13. Lewandowski, J.J. and Lowhaphandu, P. (1998). Effects of Hydrostatic Pressure on Mechanical Behavior and Deformation Processing of Materials", *International Materials Reviews,* **43(4)**, pp. 145-188.

14. Lewandowski, J.J. (1999). "Effects of the Addition of Toughening Ligaments on the Fatigue of Composites", In Fatigue '99, (X.R. Wu and Z.G. Zhang, eds.), EMAS 1998, Vol. III, pp. 1471-1477.

15. Zinsser, W.A., Solv'yev, S., and Lewandowski, J.J. (1999). "Fracture and Fatigue of Refractory Metal Intermetallic Composites", in Intermetallics VIII, Vol. 552, (E. George, M. Yamaguchi, and M. Mills, eds.), MRS, Pittsburgh, PA, pp. KK6.10.1-6.10.6.

16. Lowhaphandu, P., Montgomery, S.L., and Lewandowski, J.J. (1999). "Effects of Superposed Hydrostatic Pressure on Flow and Fracture of a Bulk Amorphous Alloy", *Scripta Metall. et Materialia,* **41(1),** pp. 19-24.

17. Lowhaphandu, P., Ludrosky, L.A., Montgomery, S.L., and Lewandowski, J.J. (1999). "Deformation and Fracture Toughness of a Bulk Amorphous Alloy", *Intermetallics,* in press.

Fatigue and Fracture Behavior of Toughened Materials

F49620-96-1-0164

John J. Lewandowski and Robert M. Aikin, Jr.
Department of Materials Science and Engineering
Case Western Reserve University
Cleveland, OH 44106

Objective:

The main focus in the present work has been on determining the fundamental mechanisms controlling the fatigue and fracture behavior of material toughened with ductile/tough phases. This research is utilizing materials processed at WPAFB form the binary Nb-Si system, as well as recently developed Nb-Ti-Hf-Si-Al-Cr (i.e. at GE CRD) base materials in order to determine the factors controlling the mechanical behavior under both monotonic and cyclic loading conditions. Considerable work has already demonstrated the positive effects of compositing Nb_5Si_3 with Nb on the toughness of such materials although relatively little is known regarding the cyclic fatigue behavior of the materials obtained from the binary Nb-Si systems as well as those obtained via alloying. A complementary AASERT program investigated the fracture and fatigue behavior of bulk metallic glasses produced at California Institute of Technology and Howmet, Inc..

Approach:

This research focused on the following areas of Nb-based toughened alloys:

1. Determining the fundamental factors controlling the fracture and fatigue behavior of the individual constituent phases which comprise toughened materials. Work on a recently completed AFOSR grant has delineated the features controlling the fracture toughness and cleavage fracture stress of unalloyed Nb and solid solution strengthened Nb-Zr and Nb-Si alloys over a range of test temperatures. The work in this grant extended such studies into Nb alloyed with Ti, Hf, Si, Al Cr and other elements as this ductile constituent. These latter alloys are being developed for improved oxidation resistance, although the effects of such alloying additions on both the fracture toughness and fatigue over a range of temperatures has not been studied to any great extent.

2. Investigation of the fatigue behavior of toughened silicides. Despite the great benefits afforded via the incorporation of ductile/tough phases into brittle materials such as Nb_5Si_3, the behavior of such systems under cyclic conditions has only recently begun to be explored and very limited data exists. Fatigue tests have been conducted under a variety of conditions in order to determine the dependence of fatigue crack growth on ΔK. All relevant portions of the fatigue crack growth curve are being developed including the threshold regime, the Paris Law regime, and the region of overload failure. Both rising ΔK and falling ΔK tests are being conducted over a range of frequencies and test temperatures in order to also determine the effects of changes in the fatigue conditions on the subsequent crack growth behavior. In addition, the effects of changes in the size and spacing of the toughening constituents on the subsequent fatigue behavior have been determined. I*n-situ* monitoring of crack growth has been used in some cases to delineate the mechanisms of crack growth.

3. Comparison of the fatigue behavior of the monolithic constituents to that of processed composites over a range of ΔK levels has been conducted. In particular, it has been determined if the mechanisms of toughening occurring in static tests are operative when testing is conducted under cyclic loading conditions. This appears to be influenced by the size of the cyclic plastic zone in relation to the microstructure (e.g. grain size) and composite architecture (e.g. size and spacing of the toughening phases).

4. The fracture and fatigue behavior of bulk metallic glass has been determined. In particular, the effects of changes in notch root radius on the magnitude of fracture toughness has been determined on both 4 mm thick plate and 7 mm thick plate supplied by Howmet, Inc. and California Institute of Technology. In addition, tension tests have been conducted with superimposed hydrostatic pressure in order to determine the effects of changes in stress state on the flow and fracture behavior.

In all cases, close contact has been maintained with researchers at WPAFB, California Institute of Technology, Howmet, Inc., and General Electric Corporate Research and Development (CE CRD). In the Nb-based systems, complementary studies are being conducted on the toughness, creep, and oxidation resistance of materials processed via vacuum arc-casting/extrusion, vapor deposition, and directional solidification. These processing forms are providing a range of microstructures and composite architectures.

SUMMARY-Fatigue of Toughened Materials

Continuing work has focused on determining the effects of cyclic loading on the fatigue crack growth behavior of both monolithic Nb and Nb alloys, as well as toughened composites. Since the start of the program in May 1996, some additional *in situ* composite materials have been obtained from GE CRD and WPAFB while additional testing has been conducted on pure Nb, binary Nb-Zr and Nb-Si materials heat treated to systematically vary the grain size.

The fatigue tests were conducted on bend bar specimens in a closed loop MTS servo-hydraulic machine at a variety of test frequencies with most at 20 Hz at a variety of R ratios including 0.05, 0.1, 0.4, 0.6 and 0.8. Data recently presented at the MRS meeting in Boston and at Fatigue '99 in China is summarized in Table I (17, 18). The data obtained on monolithic Nb shows a negligible effect of grain size on the threshold for fatigue crack growth in the Nb and Nb-Zr systems, with an improvement in threshold and fatigue behavior at higher ΔK exhibited by the Nb-Si solid solution material. Figure 1 provides data obtained on a Nb-10Si cast/extruded composite tested over a range of R-ratios. Extensive fractographic analyses have revealed that for a given R ratio, increasing the level of ΔK produces a transition in fracture mode to increasing amounts of transgranular cleavage of the primary Nb (9). Such an effect has been observed at all of the R ratios shown in Figure 1, while the quantification of the amount of cleavage present at each level of ΔK is provided in Figure 2 (9). As reviewed in recently published papers by W. Zinsser and J.J. Lewandowski (9, 11), the appearance of cleavage fracture in the Nb is probably due to the intervention of static modes of fracture at increasing values of ΔK (and K_{max}). The data in Figure 2 is replotted in Figure 3 using K_{max} as the normalizing parameter.

A possible rationale for the increase in % cleavage vs K_{max} is presented in published work (9, 11), where it is argued that the maximum extent of the plastic zone size (and hence the amount of microstructure sampled) is controlled by K_{max}. At low values of K_{max} regardless of the R ratio, the amount of primary Nb sampled by the plastic zone is insufficient to permit cleavage to occur. As K_{max} increases, the stress distribution ahead of the fatigue crack broadens and more Nb is sampled, facilitating cleavage in the primary Nb. Additional tests have been conducted at both lower and higher test temperatures in order to test the generality of such an argument. The data obtained at test temperatures as low as –125 C and as high as 225 C are shown in Figure 4. It is clear that these changes in test temperature produce increases in the fatigue crack growth rate in comparison to the data collected at room temperature shown in Figure 1. Extensive quantification of the fracture surfaces of the specimens tested at both –125 C and 225 C revealed a much higher percentage of cleavage of the primary Nb at both temperatures in comparison to the data obtained at room temperature, as shown in Figure 5, consistent with the arguments initially posed in our previous papers (9, 11).

In addition to the binary Nb-10Si composites, a variety of DS composites prepared by GE CRD have been tested. Figure 6 summarizes the effects of changes in R ratio as well as material chemistry and grain size on the threshold for fatigue on the DS materials as well as those discussed earlier. The Paris law exponents provided in Table II reveal that many of the Nb based systems and composites exhibit Paris law exponents in the range of typical metals (i.e. m=2-5). As expected, increasing the R-ratio decreases the threshold for fatigue. The mechanisms controlling fatigue and crack growth over a range of ΔK, R ratios, and test temperatures in such DS systems are being investigated concurrently. No evidence of cleavage fracture in the primary Nb has been obtained in the analysis of the quantitative fractography of the DS materials tested to date. The lack of cleavage fracture in these cases appears to be affected by the architecture of the Nb in the DS material. Extensive crack tip bifurcation has been observed with very non-planar crack fronts, suggesting that the loss of constraint accompanying such fracture events may provide one source of relaxing the local stresses sufficiently to prevent such cleavage fracture, as shown in our other work (1). The appearance of non-planar crack fronts and lack of cleavage fracture in the DS materials is also consistent with their better fatigue performance in the Paris Law regime in comparison to the Nb-10Si materials containing the same volume fraction of primary Nb.

SUMMARY- Fracture and Fatigue of Bulk Metallic Glass

The effects of changes in notch root radius on the fracture toughness of bulk metallic glass were dramatically demonstrated in recently published work by the PI (14, 20) and summarized in Figure 7. It is shown that such bulk metallic glass exhibits a fracture toughness of about 20 MPa-$m^{1/2}$ when a fatigue precrack is present, while the toughness is considerably increased (e.g. > 100 20 MPa-$m^{1/2}$) when the notch root radius is increased to only 65 μm (14,20). This effect is well in excess of that exhibited by steels and metal matrix composites in previous work conducted by the PI and his students. Figure 7 also illustrates that there is a significant increase in the amount of shear banding at the notch which accompanies the increase in toughness.

In addition, the effects of changes in the stress state on the flow and fracture of bulk metallic glass has been determined and published (16, 19). In this case, tension tests were conducted with different levels of hydrostatic pressure in an apparatus utilized by the PI in much previous work (16). It was shown that the flow/fracture stress was relatively insensitive to changes in flow stress over the range of stress states tested, in rough agreement with the von Mises yield criterion and in contrast to free volume models of flow in such materials.

References:

1. Kajuch, J., Short, J.W., and Lewandowski, J.J. (1995). "Effects of Constraint and Test Temperatures on Toughness of Nb_5Si_3/Nb Laminates", *Acta Metall. et Mater.*, **43,** pp. 1955-1967.

2. Mendiratta, M.G., Goetz, R., Dimiduk, D.M., and Lewandowski, J.J. (1995). "Unconstrained and Constrained Tensile Flow and Fracture Behavior of an Nb-1.24 at. Pct. Si Alloy", *Metall. Trans. A*, **26A**, pp. 1767-1777.

3. Rigney, J.D., and Lewandowski, J.J. (1995). "Effects of Loading Rate and Test Temperature on the Toughness of *In-Situ* Composites Based on Niobium Silicides", in *Fatigue and Fracture of Ordered Intermetallic Materials II*, (T.S., Srivatsan, W.O. Soboyejo, R.O. Ritchie, eds.), TMS, Warrendale, PA, pp. 339-359.

4. Rigney, J.D. and Lewandowski, J.J. (1996). "Fracture Toughness of Nb_5Si_3/Nb *In-situ* Composites: Part I: Loading Rate Effects", *Metall. Trans A.* **27A** pp. 3292-3306.

5. Samant, A. and Lewandowski J.J. (1997) "Effects of Grain Size and Alloy Content on the Cleavage Fracture Stress of Nb", *Metall. Trans. A*, **28A,** pp 389-399.

6. Lewandowski, J.J., Ward, C., Jackson, M.R., and Hunt, W.H., Jr., eds., *Layered Materials for Structural Applications*, MRS, Vol. 434, Pittsburgh, PA, (1996).

7. Lewandowski, J.J. and Rigney, J.D. (1996). "Temperature and Loading Rate Effects on Toughness of *In-situ* Niobium Silicide-Niobium Composites", in Proc. NATO ASI-Mechanical Behavior of Materials at High Temperature", C. Moura Branco and R.O. Rithchie, eds., NATO, Portugal, pp. 535-545.

8. Samant A. and Lewandowski, J.J. (1997). "Effects of Grain Size, Alloying Additions, and Test Temperature on Toughness of Nb", *Metall. Trans A*, **28A**, pp. 2297-2307.

9. Lewandowski, J.J. and Zinsser, W. (1998). "Effects of R-ratio on Fatigue Crack Growth of Nb-Si (ss) and Nb-10Si *In-Situ* Composites", *Metall. Trans. A.*, **29A**, pp. 1749-1757.

10. Bewlay, B., Lewandowski, J.J., and Jackson M.R. (1997). "Refractory Metal-Intermetallic *In-Situ* Composites for Aircraft Engines", *JOM,* August 1997, pp. 46-48.

11. Zinsser, W. and Lewandowski, J.J. (1998), "Fatigue Crack Growth in Nb-10Si Composites", *Scripta Metall*, **38**, 12, pp. 1775-1780.

12. Zinsser, W. and Lewandowski, J.J. (1999), "Effects of Changes in Grain Size and R-ratio on Fatigue Crack Growth of pre Nb and Nb-1 Wt % Zr", *Mater Sci. and Eng.*, Submitted.

13. Lowhaphandu, P. and Lewandowski, J.J. (1999), "Effects of Heat Treatment and Cu-Infiltration on the Toughness and Fatigue Crack Growth of Porous Steels", *Metall. Trans. A.*, 30A, pp. 325-334.

14. Lowhaphandu, P. and Lewandowski, J.J. (1998), "Fracture Toughness and Notch Toughness of Bulk Metallic Glass", *Scripta Metall*, **38**, 12, pp. 1811-1817.

15. Zwonitzer, S.A., Rozak, G. and Lewandowski, J.J. (1998) "Effects of Rolling Temperature and Reduction on Microstructure and Tensile Properties of Thick Plate, P/M Mo", In Mo and Mo Alloys, (A. Crowson, J.A. Shields, P.R. Subramainan and E.S. Chen, eds.) TMS-AIME, Warrendale, PA, pp. 111-124.

16. Lewandowski, J.J. and Lowhaphandu, P. (1998). Effects of Hydrostatic Pressure on Mechanical Behavior and Deformation Processing of Materials", *International Materials Reviews,* **43(4)**, pp. 145-188.

17. Lewandowski, J.J. (1999). "Effects of the Addition of Toughening Ligaments on the Fatigue of Composites", In Fatigue '99, (X.R. Wu and Z.G. Zhang, eds.), EMAS 1998, Vol. III, pp. 1471-1477.

18. Zinsser, W.A., Solv'yev, S., and Lewandowski, J.J. (1999). "Fracture and Fatigue of Refractory Metal Intermetallic Composites", in Intermetallics VIII, Vol. 552, (E. George, M. Yamaguchi, and M. Mills, eds.), MRS, Pittsburgh, PA, pp. KK6.10.1-6.10.6.

19. Lowhaphandu, P., Montgomery, S.L., and Lewandowski, J.J. (1999). "Effects of Superposed Hydrostatic Pressure on Flow and Fracture of a Bulk Amorphous Alloy", *Scripta Metall. et Materialia,* **41(1)**, pp. 19-24.

20. Lowhaphandu, P., Ludrosky, L.A., Montgomery, S.L., and Lewandowski, J.J. (1999). "Deformation and Fracture Toughness of a Bulk Amorphous Alloy", *Intermetallics,* in press.

Material	Grain Size (μm)	R-ratio	ΔK_{th} (MPa·m$^{0.5}$)	Paris Law Exponent, m
Nb (pure)	15(13)	0.05(13)	10.1(13)	4.2(13)
	15(13)	0.4(13)	7.1(13)	6.6(13)
	63	0.1	10.7	2.9
	63	0.4	6.6	N/A
	135	0.1	10.2	2.8
Nb-1% Zr	66	0.1	11.8	4.9
	66	0.4	7.6	N/A
	165	0.1	12.3	3.4
	165	0.4	8.6	N/A
Nb-Si(ss)	135	0.1	12.9	2.3
	135	0.4	8.1	2.5
Nb-10Si		0.05	12.0	N/A
		0.1, 0.1, 0.1	9.0, 8.4, 9.7	5.3, 6.5, 6.6
		0.4	5.6	N/A
		0.6	6.5	N/A
		0.8	4.4	N/A
DS Nb-Si-Hf-Cr-Al-Ti		0.1	8.5	2.9

TABLE 1 - FATIGUE DATA SUMMARY

Materials	Process Condition	R	ΔK_{th}, MPa$\sqrt{m}$	m	K_{IC}, MPa$\sqrt{m}$
Nb-10Si	Extruded + HT	0.05	12.0	9.1	23.4 *
	Extruded + HT	0.1	9.0	6.6	24.1 *
	Extruded + HT	0.1	8.4	6.5	24.3 *
	Extruded + HT	0.1	9.7	6.3	22.3 *
	Extruded + HT	0.6	6.5	8.9	25.4 *
	Extruded + HT	0.8	4.4	16.9	27.2 *
Nb-15Si	Extruded + HT	0.1	4.4	6.4	-
	Extruded + HT	0.4	4.1	-	-
	Extruded + HT	0.6	4.0	5.6	-
	Extruded + HT	0.8	3.7	-	16.9 *
Nb-12Si	DS	0.1	13.2	16.7	18.1
Nb-18.2Si	DS	0.1	2.5	-	3.3
Nb-30Ti-8Cr-10Al-14Si	DS	0.1	-	-	8.3 **
Nb-42.5Ti-15Si	DS	0.1	5.5	9.7	10.2
Nb-22Ti-3Hf-2Cr-2Al-17Si	Extruded + HT (1500 °C/100hr)	0.1	7.1	4.8	24.4
Nb-22Ti-3Hf-2Cr-2Al-17Si	Extruded + HT (1400 °C/100hr)	0.1	7.2	4.8	17.8

* K_{max} at fatigue overload ** Without precracking

TABLE II - FATIGUE DATA SUMMARY

CWRU

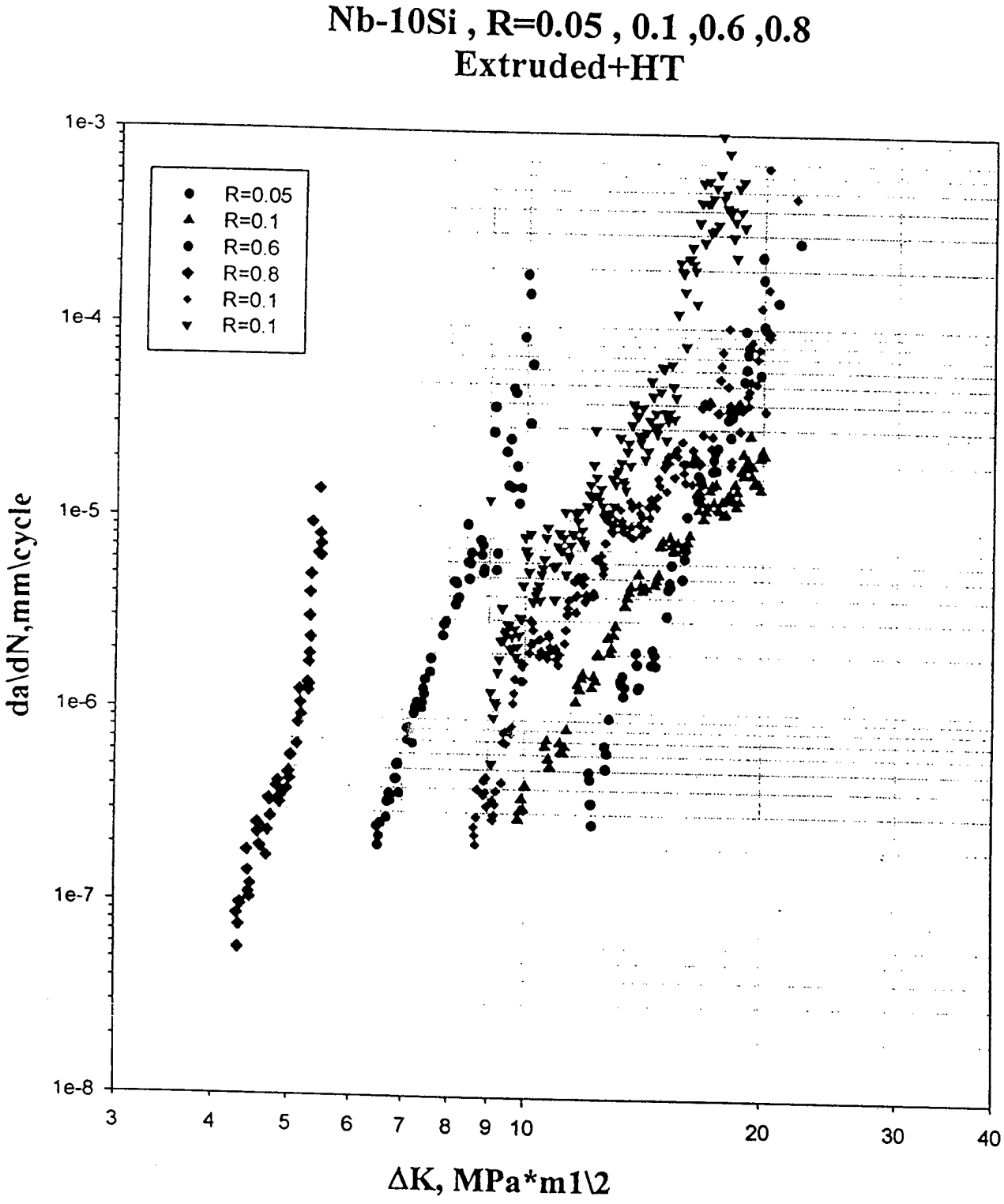

FIGURE 1. Effects of R-ratio on Fatigue Crack Growth in Nb-10Si

% Cleaved Nb_p vs. ΔK

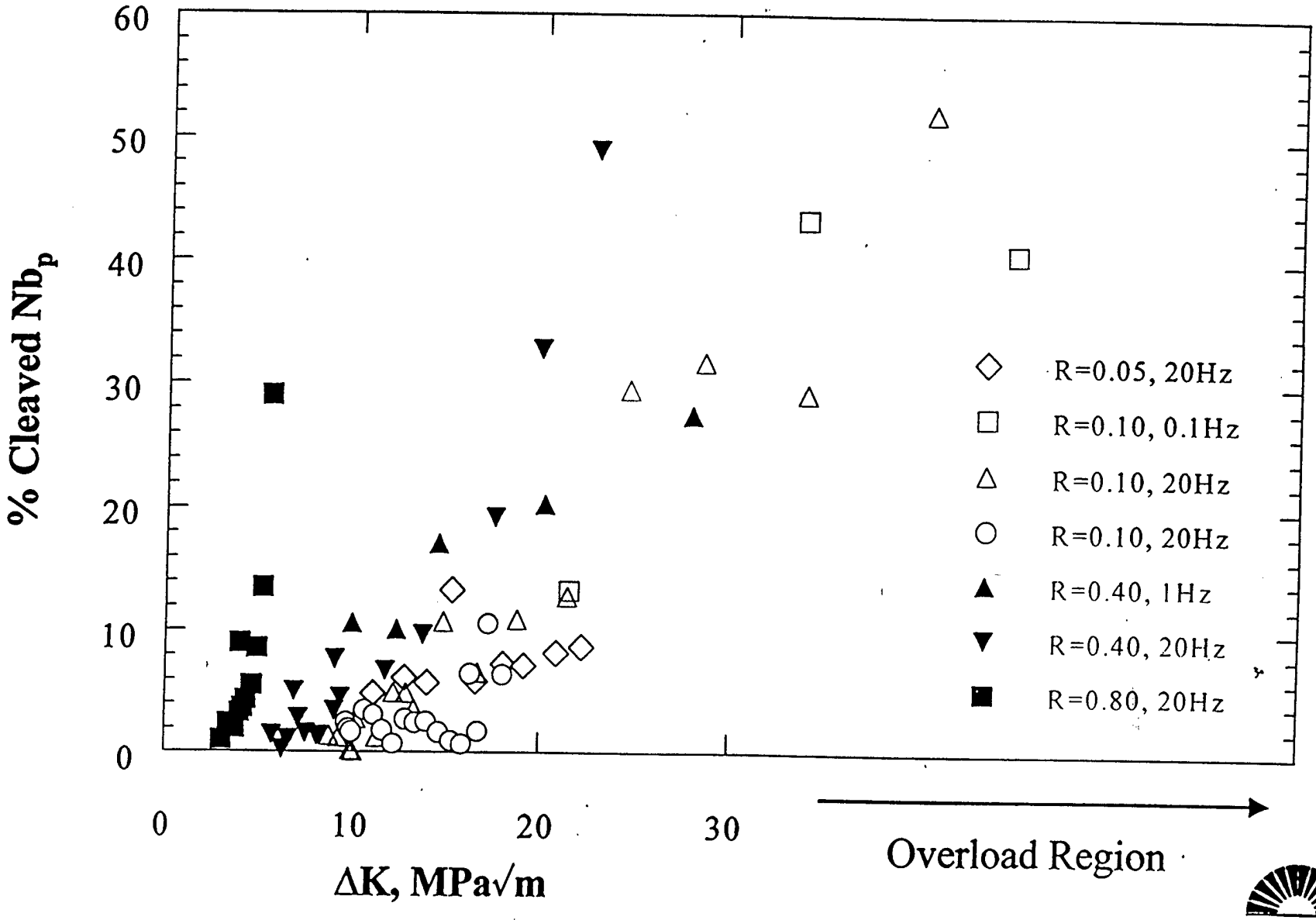

FIGURE 2. % Cleaved Primary Nb vs ΔK

CWRU

% Cleaved Nb_p vs. K_{max}

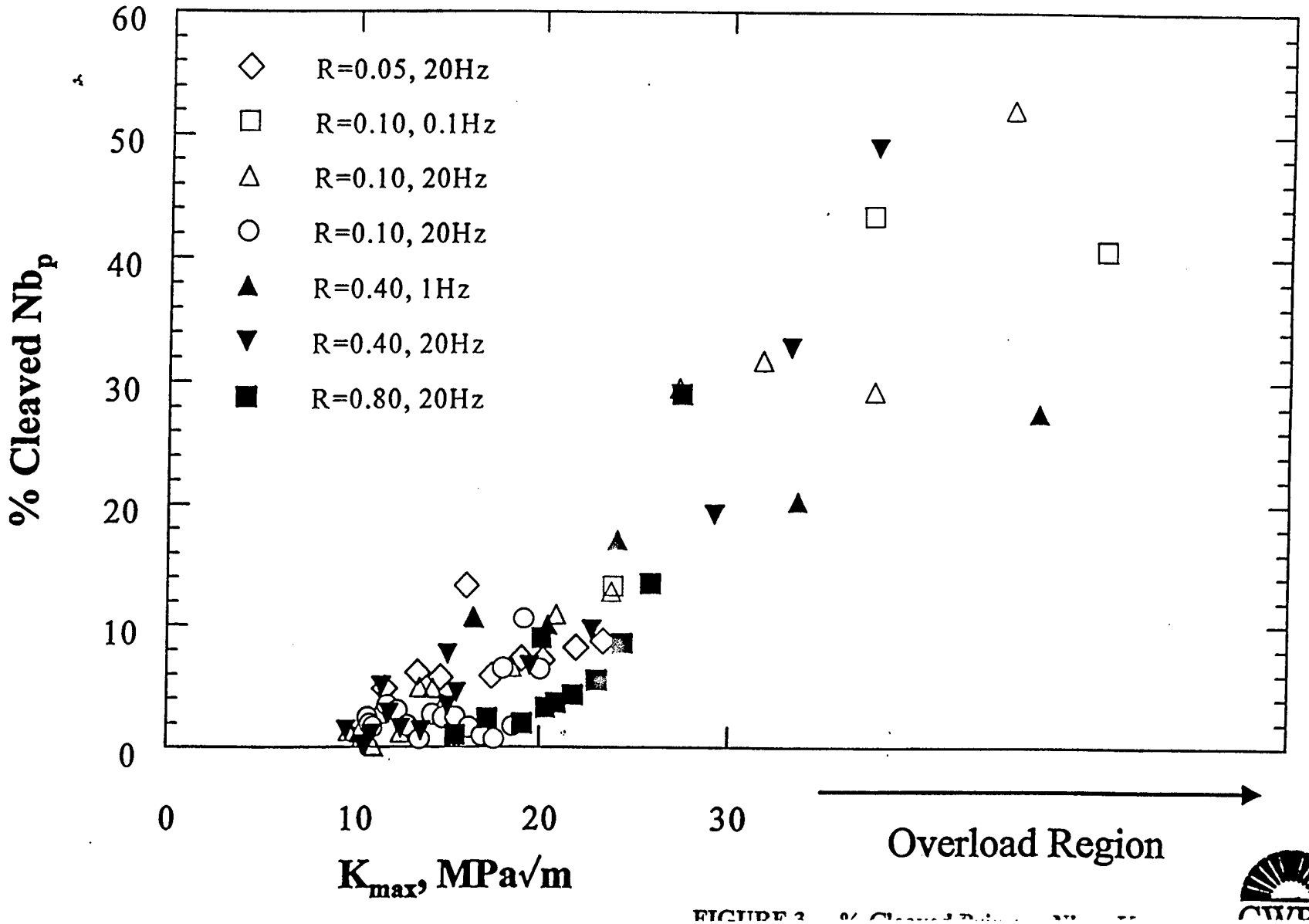

FIGURE 3 [illegible]

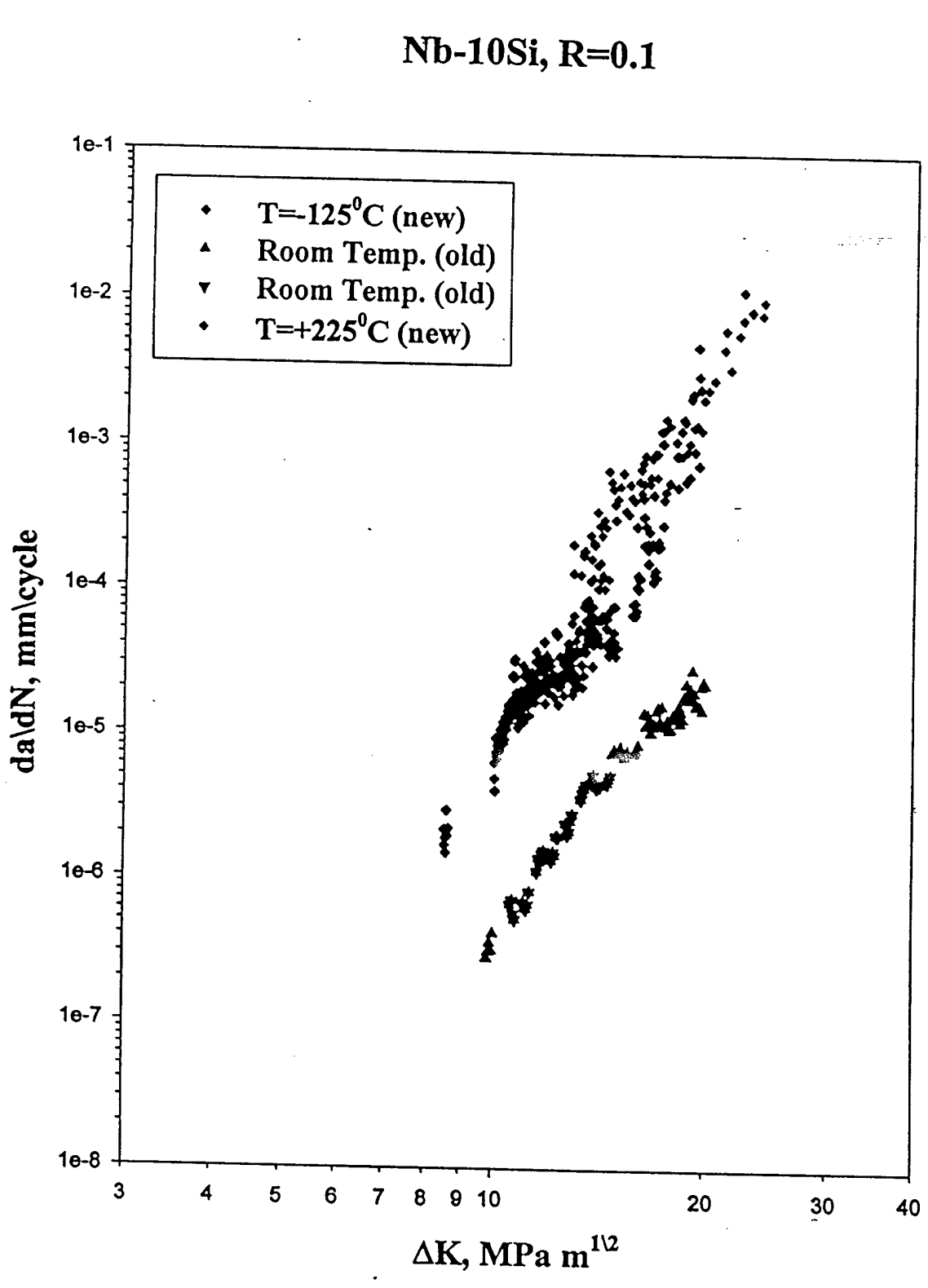

FIGURE 4. Effects of Changes in Test Temperature on Fatigue in Nb-10Si

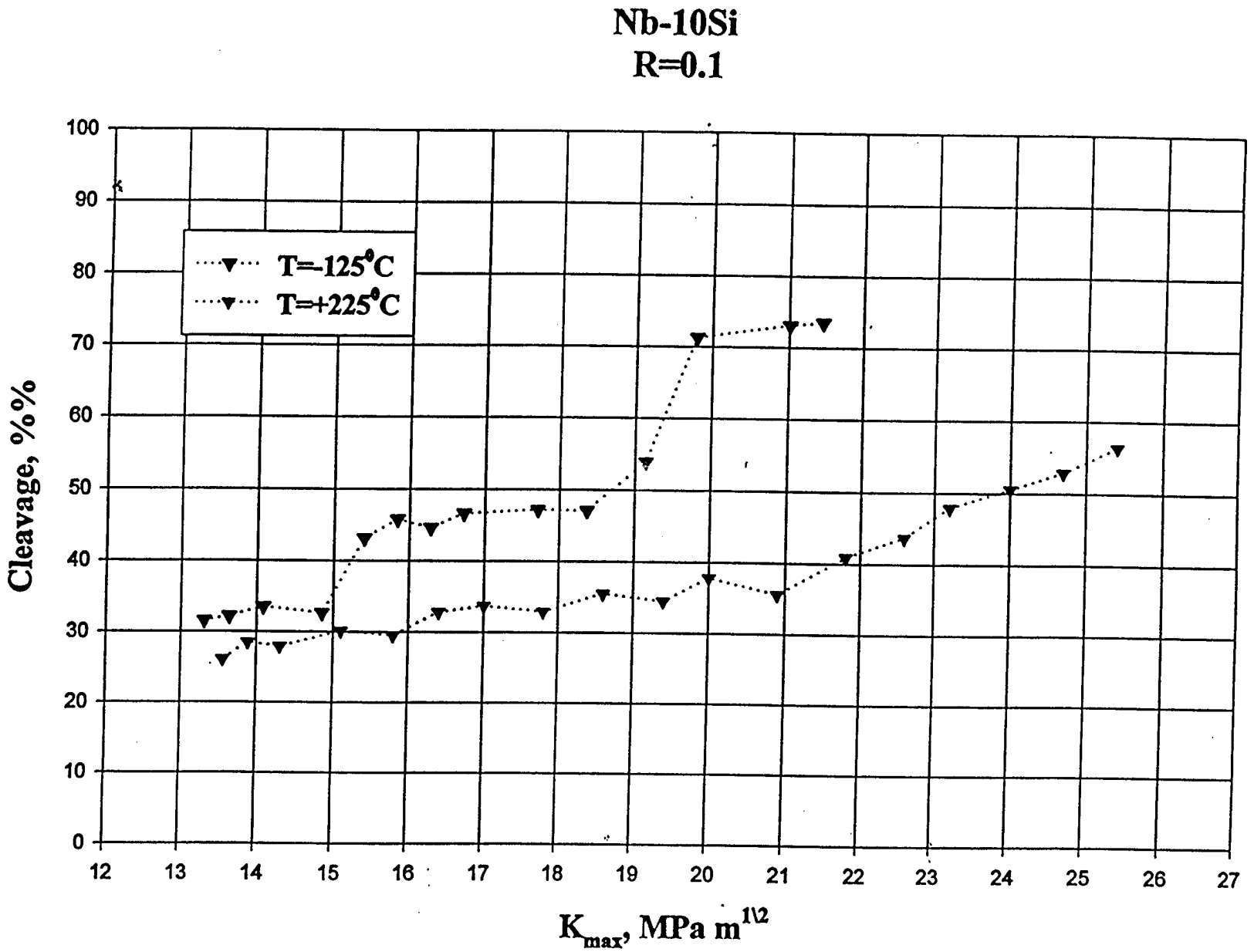

FIGURE 5. % Cleaved Primary Nb vs K_{max} for Fatigue Tests at –125C and 225C

ΔK_{th} vs. R-ratio

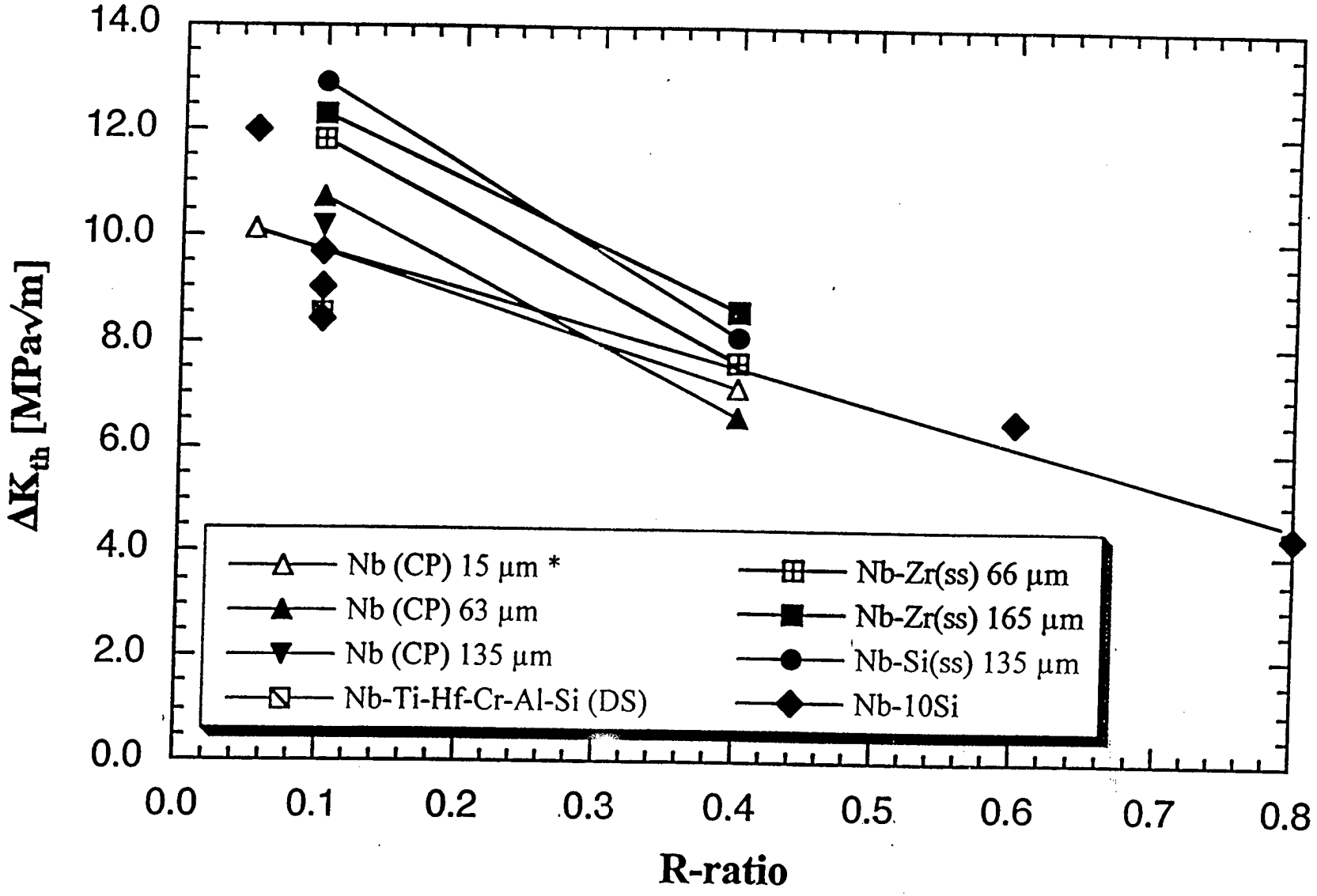

FIGURE 6. Effects of Alloy Composition, Processing Technique, and R-ratio On Fatigue Threshold

CWRU

Effects of Notch Root Radius on Fracture Profile

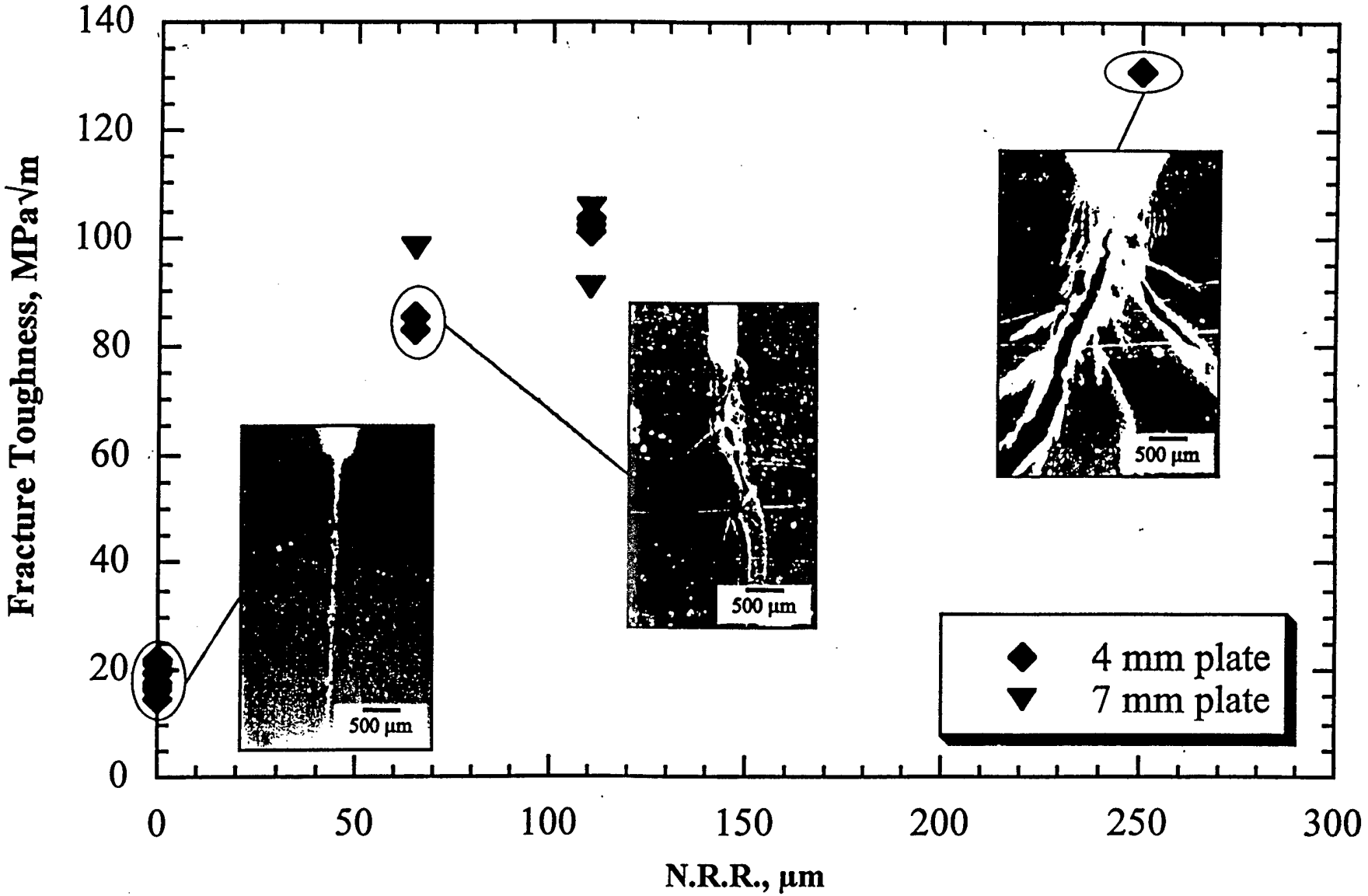

Ref: P. Lowhaphandu and J.J. Lewandowski, *Scripta Mater.*, vol. 38, no. 12, p. 1811, 1998.
P. Lowhaphandu, L.A. Ludrosky, S.L. Montgomery, and J.J. Lewandowski, *Intermetallics*, In press, 2000.

FIGURE 7. Effects of Changes in Notch Root Radius on the Fracture Profile and Toughness of Bulk Metallic Glass

CWRU

Pergamon

Scripta Materialia, Vol. 38, No. 12, pp. 1811–1817, 1998
Elsevier Science Ltd

1359-6462/98 $19.00 + .00

PII S1359-6462(98)00102-X

FRACTURE TOUGHNESS AND NOTCHED TOUGHNESS OF BULK AMORPHOUS ALLOY: Zr-Ti-Ni-Cu-Be

P. Lowhaphandu and J.J. Lewandowski
Department of Materials Science and Engineering, The Case School of Engineering,
Case Western Reserve University, Cleveland, OH 44106

(Received February 5, 1998)
(Accepted in revised form March 11, 1998)

Introduction

Recent successes in producing bulk amorphous alloys [1–4] have renewed interest in this class of materials. Although amorphous metallic alloys have been shown to exhibit strengths in excess of 2.0 GPa, most of the earlier studies on such materials were conducted on tape or ribbon specimens due to the high cooling rates required to achieve the amorphous structure. The primary purpose of this investigation was to determine the fracture toughness of a bulk metallic glass utilizing conventional procedures typically conducted with engineering materials. In particular, the effects of changes in the notch root radius from 250 μm to a fatigue precrack on the toughness were determined. It is shown presently that the average toughness obtained from six (6) fatigue precracked specimens was 18.4 ± 1.4 MPa$\sqrt{m}$, while the notch toughness obtained on specimens with notch root radii ranging from 65 μm–250 μm were in the range of 101–131 MPa$\sqrt{m}$.

Experimental Procedure

The material studied in the present investigation was supplied by Amorphous Technologies International, Inc., Laguna Niguel, California and was subsequently analyzed via wet chemistry technique to contain in wt%: 10.1Ti, 9.65Ni, 14.2Cu, 3.47Be, Balance Zr, while separate oxygen analysis revealed 1,600 ppm oxygen. The general processing details have been summarized elsewhere [1]. The material was received in the form of two separate plates of dimensions 85 mm × 65 mm × 4 mm. The structure of the material was determined on the as-received material via X-ray diffraction on a Scintag X1 apparatus using CuK_α radiation.

Fracture toughness testing was conducted in general accordance with ASTM E399 [5] on single edge notch bend specimens of nominal dimensions 85 mm × 12 mm × 4 mm or 40 mm × 8 mm × 4 mm containing notches of the following root radii: 65 μm, 110 μm, and 250 μm in addition to testing fatigue precracked specimens. In the notched toughness specimens containing notches with root radii of either 65 μm or 110 μm, the notches were placed to a depth of a/W = 0.3–0.5 using a slow speed Well vertical diamond wire saw. The 250 μm root radius notch was placed to a depth of a/W = 0.3 using a 45° V-notch cutter coated with TiN. Fatigue precracks roughly 500 μm in length were initiated from specimens with a notch root radius of 110 μm, to a depth a/W = 0.5 at an R ratio of 0.1 and

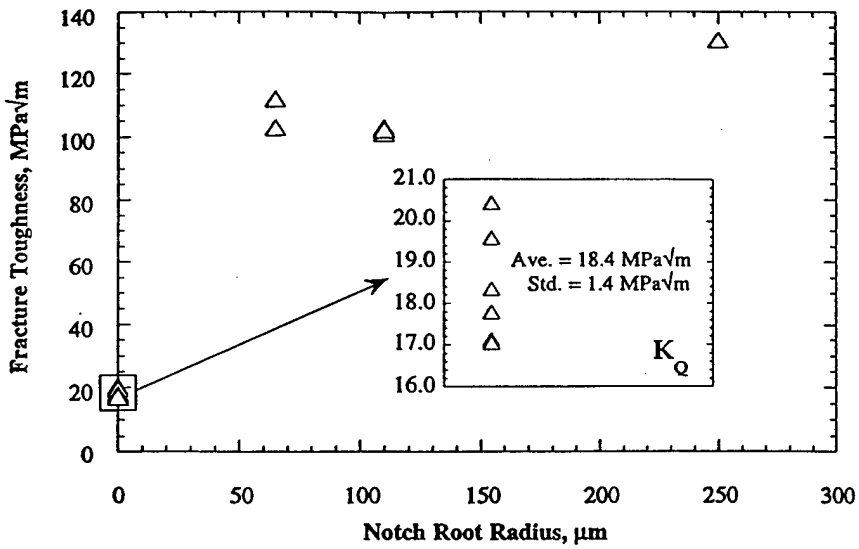

Figure 2. Notch toughness, K_Q, as a function of notch root radius. K_Q data obtained on fatigue precracked specimens (i.e., $\rho \approx 0$) are enlarged in inset box.

To the authors knowledge, these are the first reported fracture toughness values obtained on fatigue precracked bend specimens of the bulk amorphous material. There have been other recent reports [10, 11] on the toughness of similar, but not identical materials and specimen geometries. The notch bend toughness obtained on thinner (i.e., 2.2 mm thick) material was reported [10] as 57.2 ± 2.3 MPa$\sqrt{m}$, while the toughness reported [11] on somewhat thicker (i.e., 7 mm thick) fatigue precracked compact tension specimens was 55.0 ± 5.0 MPa$\sqrt{m}$. The present results [6, 7] obtained on the fatigue precracked bend specimens are significantly lower than both previous reports [10, 11] for the toughness and are lower than the notch toughness values shown in Figure 2. The apparent discrepancy between the fatigue precracked toughness values presently reported and the former report [10] on the notch toughness may be in part due to the use of a relatively blunt notch and thinner specimen (i.e. 2.2 mm) instead of the fatigue precracked thicker (i.e. 4 mm) specimen presently reported. It is known from the literature on steels [12] and metal matrix composites [13] that the notch root radius in such specimens exerts a large effect on the magnitude of the toughness measured. The present results shown in Figure 2 similarly illustrate that the measured toughness of bulk metallic glass is also significantly increased on going from a fatigue precracked specimen to that containing notches with radii of 65, 110, and 250 μm. As shown in Figure 3, the crack path profile is also significantly affected by the notch root radius. The fatigue precracked specimens exhibited a very planar crack front, Figure 3a, while the notched specimens (cf. Figure 3b, 3c) exhibited extensive shear banding at the notch as well as significant crack bifurcation once the crack propagated. Both processes (i.e., multiple shear banding, crack bifurcation) should absorb more energy than the planar fracture mode exhibited in Figure 3a, consistent with the relative differences in the measured toughness reported in Figure 2 on going from the fatigue precracked specimens to those containing somewhat blunter notches. The stress concentration and stress state ahead of a fatigue precrack is also more severe than that obtained ahead of a blunter notch. Earlier work on the notched toughness [10] of a similar bulk metallic glass also reported such crack bifurcation in a notched specimen, although fatigue precracked specimens were not tested in that work. Another factor which may contribute to this discrepancy in the magnitude of toughness measured relates to differences in the oxygen level, reported as only 800 ppm in the notch toughness study [10]. This is discussed further below.

As noted above, the present toughness data obtained on fatigue precracked bend specimens is also somewhat lower than that reported [11] on fatigue precracked compact tension specimens of a thicker

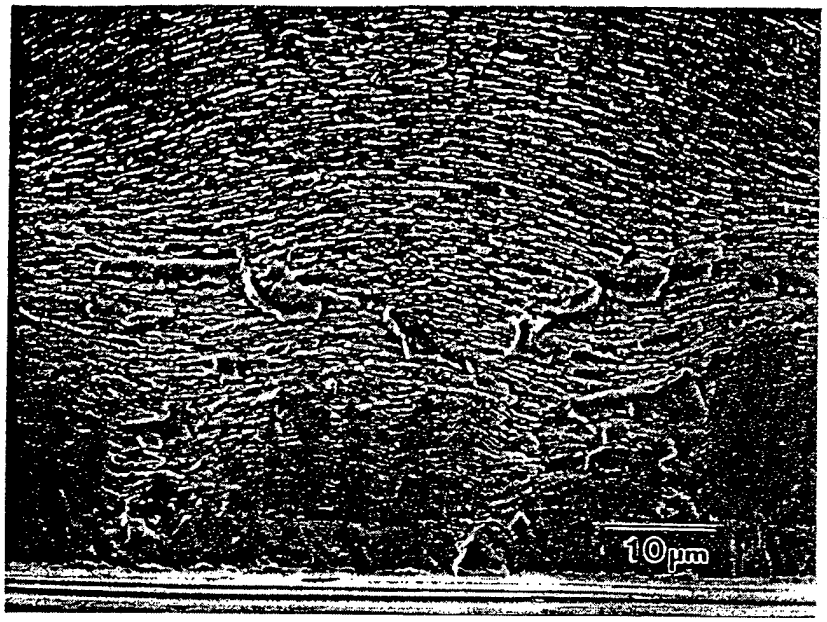

a)

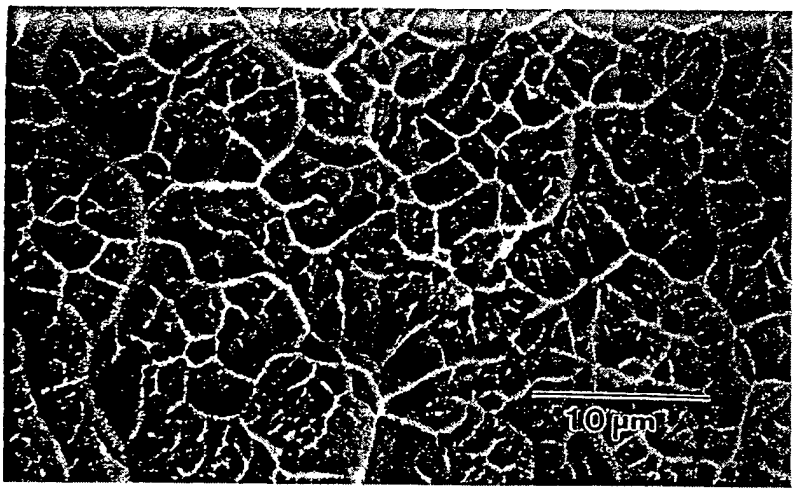

b)

Figure 4. Typical fracture surface of a fatigue precracked toughness specimen: a) fatigue striations near the notch root. Notch is at the bottom of the micrograph; b) overload region. The crack growth direction in both photos is from bottom to top.

5a. The overload region, Figure 5b, exhibited the typical vein fracture pattern reported for such materials [6, 7, 10, 11, 14, 16–18] examined at low magnification. Higher magnification views of the overload region in the notched specimens shown in Figure 5b were similar to that shown for the overload region of the fatigue precracked specimen shown in Figure 4b.

testing by L. Ludrosky is also appreciated. Discussions with Prof. Ali Argon are also gratefully acknowledged. The project is under financial support of AFOSR-AASERT F49420-96-1-0228.

References

1. A. Peker and W. L. Johnson, Appl. Phys. Lett. 63, 2342 (1993).
2. A. Inoue, T. Zhang, and T. Masumoto, Mater. Trans. Jpn. Inst. Metals. 31, 425 (1990).
3. T. Zhang, A. Inoue, and T. Masumoto, Mater. Trans. Jpn. Inst. Metals. 32, 1005 (1991).
4. A. Inoue, Y. Nakamura, N. Nishiyama, and T. Masumoto, Mater. Trans. Jpn. Inst. Metals. 33, 937 (1992).
5. ASTM E399–90: Test Method for Plane-Strain Fracture Toughness of Metallic Materials, ASTM, Philadelphia (1994).
6. P. Lowhaphandu, L. A. Ludrosky, and J. J. Lewandowski, Presented at TMS Fall Meeting, Indianapolis, IN (1997).
7. L. A. Ludrosky, P. Lowhaphandu, and J. J. Lewandowski, Nanostructured Mater. Submitted (1998).
8. S. Suresh, Fatigue of Materials, Cambridge University Press, Cambridge (1991).
9. J. F. Knott, Fundamentals of Fracture Mechanics, Butterworths, London (1973).
10. R. D. Conner, A. J. Rosakis, W. L. Johnson, and D. M. Owen, Scripta Mater. 37, 1373 (1997).
11. C. J. Gilbert, R. O. Ritchie, and W. L. Johnson, Appl. Phys. Lett. 71, 476 (1997).
12. G. R. Irwin, Appl. Mater. Res. 3, 65 (1964).
13. J. J. Lewandowski and M. Manoharan, Int. J. Fracture. 40, R31 (1989).
14. L. A. Davis, J. Mater. Sci. 10, 1557 (1975).
15. X. H. Lin, W. L. Johnson, and W. K. Rhim, Mater. Trans. JIM. 38, 473 (1997).
16. L. Q. Xing et al., Mater. Sci. Eng. A226–228, 874 (1997).
17. A. Leonard et al., Presented at TMS Annual Meeting, San Antonio, TX (1998).
18. A. S. Argon and M. Salama, Mater. Sci. Eng. 23, 219 (1976).

testing by L. Ludrosky is also appreciated. Discussions with Prof. Ali Argon are also gratefully acknowledged. The project is under financial support of AFOSR-AASERT F49420-96-1-0228.

References

1. A. Peker and W. L. Johnson, Appl. Phys. Lett. 63, 2342 (1993).
2. A. Inoue, T. Zhang, and T. Masumoto, Mater. Trans. Jpn. Inst. Metals. 31, 425 (1990).
3. T. Zhang, A. Inoue, and T. Masumoto, Mater. Trans. Jpn. Inst. Metals. 32, 1005 (1991).
4. A. Inoue, Y. Nakamura, N. Nishiyama, and T. Masumoto, Mater. Trans. Jpn. Inst. Metals. 33, 937 (1992).
5. ASTM E399–90: Test Method for Plane-Strain Fracture Toughness of Metallic Materials, ASTM, Philadelphia (1994).
6. P. Lowhaphandu, L. A. Ludrosky, and J. J. Lewandowski, Presented at TMS Fall Meeting, Indianapolis, IN (1997).
7. L. A. Ludrosky, P. Lowhaphandu, and J. J. Lewandowski, Nanostructured Mater. Submitted (1998).
8. S. Suresh, Fatigue of Materials, Cambridge University Press, Cambridge (1991).
9. J. F. Knott, Fundamentals of Fracture Mechanics, Butterworths, London (1973).
10. R. D. Conner, A. J. Rosakis, W. L. Johnson, and D. M. Owen, Scripta Mater. 37, 1373 (1997).
11. C. J. Gilbert, R. O. Ritchie, and W. L. Johnson, Appl. Phys. Lett. 71, 476 (1997).
12. G. R. Irwin, Appl. Mater. Res. 3, 65 (1964).
13. J. J. Lewandowski and M. Manoharan, Int. J. Fracture. 40, R31 (1989).
14. L. A. Davis, J. Mater. Sci. 10, 1557 (1975).
15. X. H. Lin, W. L. Johnson, and W. K. Rhim, Mater. Trans. JIM. 38, 473 (1997).
16. L. Q. Xing et al., Mater. Sci. Eng. A226–228, 874 (1997).
17. A. Leonard et al., Presented at TMS Annual Meeting, San Antonio, TX (1998).
18. A. S. Argon and M. Salama, Mater. Sci. Eng. 23, 219 (1976).

Pergamon

Scripta Materialia, Vol. 41, No. 1, pp. 19–24, 1999
Elsevier Science Ltd

1359-6462/99/$–see front matter

PII S1359-6462(99)00128-1

EFFECTS OF SUPERIMPOSED HYDROSTATIC PRESSURE ON FLOW AND FRACTURE OF A Zr-Ti-Ni-Cu-Be BULK AMORPHOUS ALLOY

P. Lowhaphandu, S.L. Montgomery, and J.J. Lewandowski
Department of Materials Science and Engineering, The Case School of Engineering, Case Western Reserve University, Cleveland, OH 44106

(Received April 13, 1999)
(Accepted April 16, 1999)

Keywords: Amorphous materials; Fracture; Shear bands

Introduction

Recent successes in producing bulk amorphous alloys (1–4) have renewed interest in this class of materials. Although amorphous metallic alloys have been shown to exhibit strengths in excess of 2.0 GPa, most of the earlier studies on such materials were conducted on tape or ribbon specimens due to the high cooling rates required to achieve the amorphous structure. The primary purpose of this investigation was to determine the effects of superimposed hydrostatic pressure on the flow and fracture behavior of a Zr-Ti-Ni-Cu-Be bulk metallic glass utilizing procedures successfully utilized on a range of structural materials, as reviewed recently (5). In general, few studies of this type have been conducted on metallic glasses, although thin ribbons (i.e., 300 μm thick) of a Pd-Cu-Si amorphous material tested with superimposed pressure have been reported previously (6).

In particular, the effects of superimposed hydrostatic pressure over levels ranging from 50 MPa to 575 MPa on the flow/fracture behavior of cylindrical tensile specimens were compared to the flow and fracture behavior of identical materials tested in uniaxial tension and compression. It is shown that changes in stress triaxiality, defined as $\sigma_m/\bar{\sigma}$, over the range of -0.33 to 0.33 produced a negligible effect on the fracture stress and fracture strain, while the orientation of the macroscopic fracture plane with respect to the loading axis was significantly affected by changes in $\sigma_m/\bar{\sigma}$.

Experimental Procedure

The material studied in the present investigation was supplied by Amorphous Technologies International, Inc., Laguna Niguel, California and was subsequently analyzed via wet chemistry technique (by Herron Testing Laboratories, Inc., Cleveland, OH) to contain in wt%: 9.9Ti, 9.4Ni, 13.4Cu, 4.1Be, Balance Zr, while separate oxygen analyses revealed 1,300/1,400 ppm oxygen. The general processing details have been summarized elsewhere (1). The material was received in the form of a 7.6 mm-thick plate of dimensions 105 mm × 145 mm. The structure of the material was confirmed to be amorphous via X-ray diffraction on a Scintag X1 apparatus using CuK_α radiation, as shown previously on similar

material processed as 4 mm-thick plate (7) on which fracture toughness measurements have been reported.

The as-received plate was electrical discharge machined (EDM) into square cross-section blank bars of nominal dimensions: 7.6 mm × 7.6 mm × 90 mm. Both compression specimens and tension specimens were machined from these blank bars using carbide tools. The cylindrical compression specimens were nominally 12.7 mm in length and 6.35 mm in diameter, providing a nominal length-to-diameter aspect ratio of 2:1 as recommended by ASTM E8-89 for testing high strength material. The compression specimens were ground using SiC grinding papers followed by polishing with diamond paste to a 0.25 μm finish. The button-head tension specimens were first machined according to dimensions provided for sub-size specimens in ASTM E9M-94a. The tension specimens had a nominal gage diameter of 3.0 mm and gage length 12.5 mm. The gage section of each specimen was polished to a 0.25 μm finish using a combination of SiC grinding papers and diamond paste.

Compression tests at 1 atm (i.e., pressure of 0.1 MPa) were conducted on a 50 kip MTS servohydraulic testing machine under displacement-control mode. Compression anvils made of hardened tool steel with hardness in excess of that of the bulk metallic glass were utilized in order to minimize deformation of the anvils. Friction between the compression anvils and specimens was minimized via the use of MoS_2 lubricant. The displacement rate was chosen to provide an initial strain rate of 10^{-4} sec^{-1} as specified by ASTM E8-89. Tension tests at 1 atm (i.e., 0.1 MPa) were conducted at 10^{-3} sec^{-1} using two machines: 1) an Instron Universal Testing Machine Model 1125 outfitted with high alignment grips; and 2) a High Pressure Deformation Apparatus operated at 1 atm in the CWRU High Pressure Laboratory. Separate tension tests were also conducted with different (i.e., higher) levels of confining (i.e., gas) pressure using the latter apparatus, which consists of a compound pressure vessel, 2-stage pressurization system, 110 kip MTS servohydraulic actuator, various diagnostics for load, pressure, and displacement in addition to a data acquisition system. The pressurization fluid used was industrial-grade argon, while other features of the apparatus are described elsewhere (5). The tension specimens were placed into the load train assembly and inserted into the pressure vessel prior to pressurization. The pressurization rate did not exceed 50 MPa/min. Upon reaching the desired pressure, the specimens were held at that pressure for at least five minutes before being tested under constant displacement rate, which provided an initial strain rate of 10^{-3} sec^{-1}, in accordance with ASTM E9M-94a. Load, measured on a pressure-compensated load cell mounted on the load train assembly inside the pressure vessel, was continuously monitored to the point of specimen failure, as was displacement and confining pressure. The fracture stress for each specimen was calculated as the maximum load sustained divided by the minimum cross sectional area.

The fractured specimens were examined both macroscopically and microscopically. The macroscopic fracture plane angle (with respect to the loading axis) was measured by a Bausch & Lomb contour measuring projector for each specimen tested. The fracture surfaces of all specimens were examined using a Hitachi S4500 Field Emission Scanning Electron Microscope (SEM) and a Leica Wild M8 zoom stereomicroscope.

Results

All specimens tested exhibited load vs. displacement traces which were linear to failure. The tension specimens tested at 1 atm (i.e., 0.1 MPa) exhibited fracture surfaces which were oriented nominally perpendicular to the tensile axis, as shown in Figure 1a. Multiple fragments were exhibited by such tests and all surfaces were (nominally) macroscopically perpendicular to the tensile axis and well removed from the specimen shoulders. All other specimens (i.e., compression, tension with confining pressure) exhibited fracture surfaces which were clearly oriented at some angle to the tensile axis, as shown in

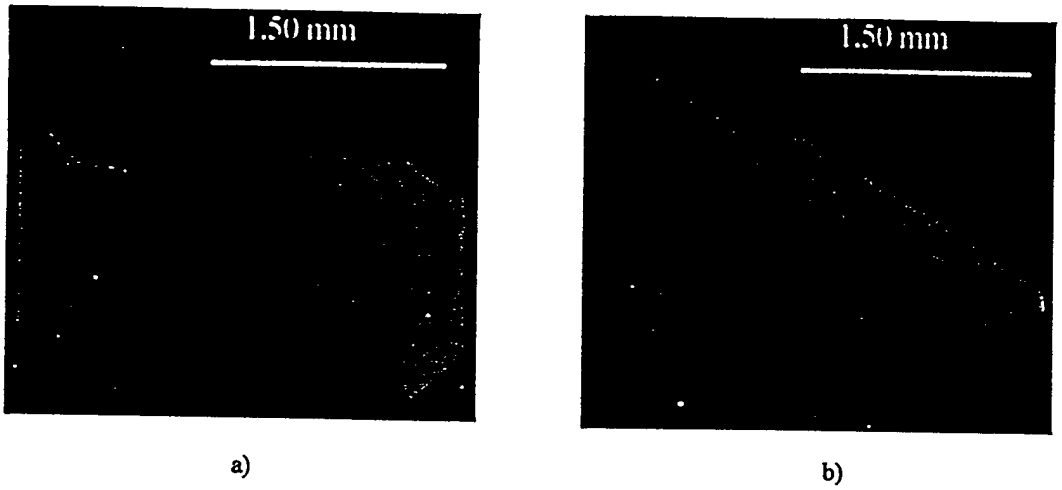

Figure 1. Typical failure mode of: a) Tension specimens tested at 1 atm; b) Tension specimens tested with superimposed hydrostatic pressure. Compression specimens tested at 1 atm exhibited similar macroscopic features as (b), although at a different angle to the loading axis.

Figure 1b. Nonpropagating microcracks/shear bands parallel to the fracture surface were also observed in those specimens. Fracture again occurred within the gage length and well removed from the loading fixtures in all but one specimen out of a total of 13 specimens tested.

Figure 2 illustrates the large effects of stress state (i.e., tension, compression, and level of superimposed pressure) on the macroscopic orientation of the fracture surface with respect to the loading axis. The average angle between the macroscopic fracture plane and the loading axis in the compression specimens was 41.6° ± 2.1°, while that of the tension specimens tested with superimposed hydrostatic pressure between 50 MPa to 575 MPa was 57.0° ± 3.7°. Both values are significantly different from those reported on thin ribbons of amorphous alloys, which exhibited nominally 45° (6,8,9). Figure 3 summarizes the relatively minor effect of superimposed pressure on the flow/fracture stress, over the range of conditions tested. The average tensile fracture stress obtained on 3 specimens tested at 0.1 MPa was 1978 ± 20 MPa, while that obtained in three specimens tested in compression was 1911 ± 64 MPa. The slightly higher scatter in fracture stress exhibited by the compression specimens could in part be due to residual polishing scratches noticed on the surface of the specimen which exhibited the lowest fracture stress. The seven tension tests conducted with confining pressure exhibited a fracture stress of

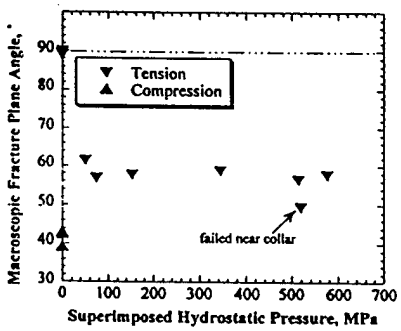

Figure 2. Macroscopic fracture plane angle as a function of superimposed hydrostatic pressure.

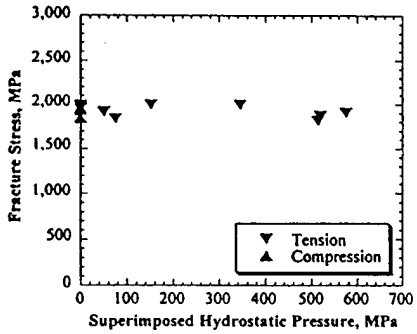

Figure 3. Fracture stress as a function of superimposed hydrostatic pressure.

1910 ± 71 MPa. Neither tension testing with superimposed pressure nor compression testing produced a significant change in the macroscopic fracture strain, which was essentially zero for all the conditions presently tested.

Discussion

The effects of superimposed pressure on a variety of materials have recently been reviewed (5). A convenient way to analyze the present results is to replot all of the data presented in Figures 2 and 3 vs. the level of stress triaxiality (χ), defined as $\chi = \sigma_m/\bar{\sigma}$ where σ_m $(=(\sigma_1 + \sigma_2 + \sigma_3)/3)$ is the mean stress and $\bar{\sigma}$ $(= \sqrt{2}/2[(\sigma_1 - \sigma_2)^2 + (\sigma_2 - \sigma_3)^2 + (\sigma_3 - \sigma_1)^2]^{1/2})$ is the effective stress. Figure 4 replots the values presented in Figure 2 for the macroscopic orientation of the fracture plane to the loading axis vs. level of stress triaxiality, χ. The data in Figure 4 reveal an effect of stress triaxiality on the macroscopic orientation of the fracture surface, although Figure 5 indicates relatively little effect of triaxiality, over the range measured, on the magnitude of the flow/fracture stress. The fracture strain was essentially zero for all of the conditions tested.

Previous work on a similar bulk metallic glass tested in uniaxial tension, compression, and torsion, suggested that the flow/fracture behavior of such materials obeyed a von Mises criterion which provides for pressure-independent behavior (10). The present work has employed various levels of superimposed hydrostatic pressure in order to independently vary the level of triaxiality present in tension tests over the range $\sigma_m/\bar{\sigma} = -0.33$ to 0.33. In the present work, a negligible effect of confining pressure on the flow/fracture stress was obtained, Figure 3, consistent with pressure-independent behavior as predicted

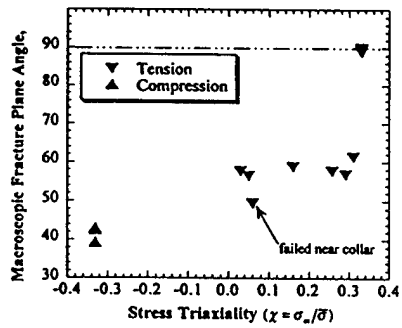

Figure 4. Macroscopic fracture plane angle as a function of stress triaxiality ($\chi = \sigma_m/\bar{\sigma}$).

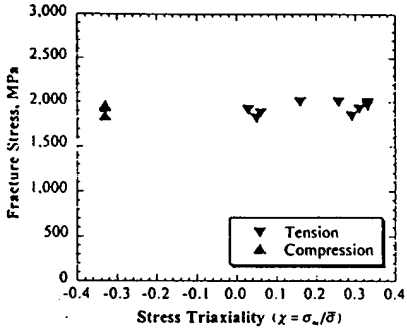

Figure 5. Fracture stress as a function of stress triaxiality ($\chi = \sigma_m/\bar{\sigma}$).

by the von Mises criterion. This is somewhat in contrast to the work conducted on thin ribbons of amorphous Pd-Cu-Si (6) where a slight pressure dependence of the flow/fracture behavior was reported, although attempts at distinguishing between a pressure dependent yield criterion or a Mohr-Coulomb type criterion was not possible in that work. However, the work on the thin ribbons (6) also noted that there may have been problems with alignment and gripping which facilitated deformation and fracture at the grip ends as opposed to within the gage length. The present results are also somewhat in contrast to various models of flow in amorphous materials which predict a pressure dependence to the flow behavior (11). Localized flow and subsequent/concomitant shear banding has been modeled in such materials as due to a decrease in viscosity resulting from local dilatation of the glass in regions of high tensile stress (12,13). Such models based on "free volume" or "dilatation" have been developed and successfully used in the quantitative treatment of high temperature viscous deformation (14), while the transition to localized flow at low temperatures is also qualitatively consistent with such a mechanism. However, while the formation of a localized shear band presumably occurs via the accumulation of free volume created during the shearing of small groups of atoms, such a mechanism should be dependent on the hydrostatic component of applied stress (15). The present work clearly illustrates that the pressure dependence of the flow stress in this bulk metallic glass over the range measured is not significantly greater than that of homogeneous and isotropic crystalline cubic metals, as reviewed recently (5). In support of this apparent lack of pressure dependence to the flow/fracture stress observed presently, the difference between the uniaxial tensile strength and compressive strength is also small in the present study.

Kimura and Masumoto have similarly reported that amorphous $Pd_{77.5}Cu_6Si_{16.5}$ follows a von Mises yield criterion, consistent with a flow criterion that is dominated by shear processes (16,17). Donovan's work on amorphous $Pd_{40}Ni_{40}P_{20}$ (18) also suggested that plastic flow had negligible dependence on pressure from experiments conducted in compression, plane-strain compression, tension, and pure shear. The present work conducted with different levels of superimposed hydrostatic pressure directly tests such hypotheses and is in agreement that superimposed pressure (over the range tested) produces a negligible effect on the flow/fracture stress.

While it is clear that superimposed pressure and changes in stress triaxiality (over the range tested) have little effect on the flow/fracture stress and fracture strain in the Zr-Ti-Ni-Cu-Be bulk metallic glass tested presently, a relatively strong normal stress dependence was demonstrated by the macroscopic orientation of the fracture plane as shown in Figures 2 and 4. Deviation of the fracture plane away from the maximum shear plane (i.e., 45°) is an indication that the flow process of the material has a dependency on the normal stress acting on the shear plane. Such observations in the past by Donovan (18) have been utilized to support a pressure-modified Mohr-Coulomb yield criterion of the form

$$\tau_c = k_0 - \alpha\sigma_n - \beta(\sigma_1 + \sigma_2 + \sigma_3)/3$$

where τ_c is the shear stress on the slip plane at yielding, σ_n is the stress component in the direction normal to the slip plane, and α, k_0, and β are constants. The present results for the Zr-Ti-Ni-Cu-Be glass strongly suggest that the pressure sensitivity term, β, is negligible over the range measured. While the macroscopic orientation of the fracture plane is clearly affected by the loading conditions, Figures 2 and 4, there is negligible tension/compression asymmetry to the flow/fracture behavior, as shown in Figures 3 and 5. Experiments are being conducted over a wider range of stress triaxiality and normal stress in order to resolve the contributions to this apparent internal inconsistency in observations. Finally, the present observations are not necessarily inconsistent with results obtained on some other materials such as polymers, soils, and rocks which all exhibit normal-stress dependency to some extent and widely different pressure sensitivities.

Conclusion

1) The flow/fracture stress and fracture strain of Zr-Ti-Ni-Cu-Be bulk amorphous alloy is negligibly affected by changes in stress triaxiality over the range $\sigma_m/\bar{\sigma} = -0.33$ to 0.33 and is essentially independent of superimposed hydrostatic pressure over the range 50 MPa to 575 MPa.
2) The macroscopic orientation of the fracture plane relative to the stress axis was strongly affected by changes in stress triaxiality, suggesting normal stress dependence to the flow/fracture behavior, although little tension/compression asymmetry to the flow/fracture stress was obtained. Experiments over a wider range of stress states are underway in order to resolve this apparent inconsistency.

Acknowledgments

The authors gratefully acknowledge the supply of material by Drs. Atakan Peker and Michael Tenhover of Amorphous Technologies International, Inc. (ATI) and helpful interactions with Dr. W.L. Johnson (Keck Laboratory of Engineering Materials, California Institute of Technology). Discussions with Prof. Ali Argon and Prof. Frans Spaepen are also gratefully acknowledged. The project is under financial support of AFOSR-AASERT F49420-96-1-0228.

References

1. A. Peker and W. L. Johnson, Appl. Phys. Lett. 63, 2342 (1993).
2. A. Inoue, T. Zhang, and T. Masumoto, Mater. Trans. Jpn. Inst. Metals. 31, 425 (1990).
3. T. Zhang, A. Inoue, and T. Masumoto, Mater. Trans. Jpn. Inst. Metals. 32, 1005 (1991).
4. A. Inoue, Y. Nakamura, N. Nishiyama, and T. Masumoto, Mater. Trans. Jpn. Inst. Metals. 33, 937 (1992).
5. J. J. Lewandowski and P. Lowhaphandu, Intr. Mater. Rev. 43, 145 (1998).
6. L. A. Davis and S. Kavesh, J. Mater. Sci. 10, 453 (1975).
7. P. Lowhaphandu and J. J. Lewandowski, Scripta Mater. 38, 1811 (1998).
8. H. J. Leamy, H. S. Chen, and T. T. Wang, Metall. Trans. 3, 699 (1972).
9. C. A. Pampillo and D. E. Polk, Acta Metall. 22, 741 (1994).
10. H. A. Bruck, T. Christman, A. J. Rosakis, and W. L. Johnson, Scripta Metall. 30, 429 (1994).
11. F. Spaepen and D. Turnbull, Scripta Metall. 8, 563 (1974).
12. F. Spaepen, Acta Metall. 25, 407 (1977).
13. A. S. Argon, Acta Metall. 27, 47 (1979).
14. A. S. Argon and L. T. Shi, Acta Metall. 31, 499 (1983).
15. P. S. Steif, J. Mech. Phys. Solids. 31, 359 (1983).
16. H. Kimura and T. Masumoto, Acta Metall. 28, 1663 (1980).
17. H. Kimura and T. Masumoto, Acta Metall. 28, 1677 (1980).
18. P. E. Donovan, Acta Metall. 37, 445 (1989).

ELSEVIER

Intermetallics 0 (2000) 1–6

Intermetallics

Deformation and fracture toughness of a bulk amorphous Zr–Ti–Ni–Cu–Be alloy

P. Lowhaphandu, L.A. Ludrosky, S.L. Montgomery, J.J. Lewandowski *

Department of Materials Science and Engineering, The Case School of Engineering, Case Western Reserve University, Cleveland, OH 44107, USA

Abstract

The flow behavior and fracture toughness of two different plate thicknesses (i.e. 4 and 7 mm) of a bulk amorphous Zr–Ti–Ni–Cu–Be alloy was investigated. It is shown that the flow/fracture stress was independent of superimposed hydrostatic pressure over the range 50–575 MPa, suggesting that the flow behavior follows the von Mises criterion. However, the macroscopic orientation of the fracture plane relative to the stress axis was strongly affected by changes in stress state, suggesting some normal stress dependence to the flow/fracture behavior. The fracture behavior was also studied on both notched and precracked bend bars for both plate thicknesses. The average fracture toughness obtained from seven fatigue precracked specimens taken for both plate thicknesses was 17.9 ± 1.8 MPa$\sqrt{m}$, while the notched toughness obtained on specimens with notch root radii ranging from 65 to 250 μm taken from both plate thicknesses were in the range of 91–131 MPa$\sqrt{m}$.

Keywords: B. Fracture toughness; B. Fracture stress

1. Introduction

Recent successes in producing bulk amorphous alloys (i.e. metallic glasses) [1–4], have resulted in extensive investigations on the processing techniques/parameters, the decomposition/crystallization process, as well as the effects of nanocrystalline phase formation on the mechanical properties. A few studies have been conducted on the mechanical properties of fully amorphous materials [5–12]. In this study, the effects of changes in stress state, conducted via utilizing different loading configurations (e.g. compression vs. tension) and superimposed hydrostatic pressure, on the flow behavior has been determined. In addition, the effects of changes in notch root radius from fatigue precracked to 250 μm on the fracture toughness of a bulk Zr–Ti–Ni–Cu–Be alloy were determined.

2. Experimental procedures

2.1. Materials

The materials used in this investigation were supplied by Amorphous Technologies International, Inc., Laguna Niguel, CA. Three plates of bulk amorphous Zr–Ti–Ni–Cu–Be alloy (Vitreloy™) were received: two 4 mm-thick plates and one 7 mm-thick plate. The composition of the as-received plates were subsequently analyzed via wet chemistry technique (by Stork Herron Testing Laboratory, Inc., Cleveland, OH) to contain in wt %: 10.1 Ti, 9.6 Ni, 14.2 Cu, 3.5 Be, and Balance Zr for 4 mm-thick material and 9.9 Ti, 9.4 Ni, 13.4 Cu, 4.1 Be, and Balance Zr for 7 mm-thick material. Separate oxygen analyses revealed 1600 wppm and 1350 wppm oxygen for 4 mm and 7 mm material respectively. The general processing details have been summarized elsewhere [1]. The structure of the as-received materials were confirmed to be amorphous via X-ray diffraction on a Scintag X1 apparatus using CuK_α radiation and differential scanning calorimetry (DSC) on a TA Instrument DSC 2920 using a heating rate of 20 K/min.

2.2. Mechanical testing

2.2.1. Compression and tension tests

The flow behavior was evaluated via uniaxial compression and tension tests on the 7 mm-thick material. The cylindrical compression specimens were nominally 12.7 mm in length and 6.35 mm in diameter, providing a nominal length-to-diameter aspect ratio of 2:1 as recommended by ASTM E9-89a for testing high

* Corresponding author. Tel.: +1-216-368-4234; fax: +1-216-368-3209.

0966-9795/00/$ - see front matter
PII: S0966-9795(99)00137-5

strength material. The compression specimens were ground using SiC grinding papers followed by polishing with diamond paste to a 0.25 μm finish. The button-head tension specimens were first machined according to dimensions provided for sub-size specimens in ASTM E8-95a. The tension specimens had a nominal gage diameter of 3.0 mm and gage length 12.5 mm. The gage section of each specimen was polished to a 0.25 μm finish using a combination of SiC grinding papers and diamond paste.

Compression tests at 1 atm (i.e. pressure of 0.1 MPa) were conducted on a 50 kip MTS servohydraulic testing machine under displacement-control mode. Compression anvils made of hardened tool steel with hardness in excess of that of the bulk metallic glass were utilized in order to minimize deformation of the anvils. Friction between the compression anvils and specimens was minimized via the use of MoS_2 lubricant. The displacement rate was chosen to provide an initial strain rate of 10^{-4} s^{-1} as specified by ASTM E9-89a. The fracture stress for each specimen was calculated as the maximum load sustained divided by the cross-sectional area.

Tension tests at 1 atm (i.e. 0.1 MPa) were conducted at 10^{-3} s^{-1} using two machines: (1) an Instron Universal testing machine Model 1125 outfitted with high alignment grips; and (2) a high pressure deformation apparatus operated at 1 atm in the CWRU high pressure laboratory. Separate tension tests were also conducted with different (i.e. higher) levels of confining (i.e. gas) pressure using the latter apparatus, which consists of a compound pressure vessel, 2-stage pressurization system, 110 kip MTS servohydraulic actuator, various diagnostics for load, pressure, and displacement in addition to a data acquisition system. The pressurization fluid used was industrial-grade argon, while other features of the apparatus are described elsewhere [13]. The tension specimens were placed into the load train assembly and inserted into the pressure vessel prior to pressurization. The pressurization rate did not exceed 50 MPa/min. Upon reaching the desired pressure, the specimens were held at that pressure for at least 5 min before being tested under constant displacement rate, which provided an initial strain rate of 10^{-3} s^{-1}, in accordance with ASTM E8-95a. Load, measured on a pressure-compensated load cell mounted on the load train assembly inside the pressure vessel, was continuously monitored to the point of specimen failure, as was displacement and confining pressure. The fracture stress for each specimen was calculated as the maximum load sustained divided by the minimum cross-sectional area.

2.2.2. *Fracture toughness tests*

Fracture toughness testing was conducted in general accordance with ASTM E399-90 on single edge notch bend specimens of nominal dimensions 85×12×4 mm or 40×8×4 mm for specimens taken from plate that was 4 mm thick and 95×14×7.5 mm for specimens taken from a plate that was 7 mm thick. Notches with the following root radii were utilized: 65, 110 and 250 μm in addition to testing fatigue precracked specimens. In the notched toughness specimens containing notches with root radii of either 65 or 110 μm, the notches were placed to a depth of a/W = 0.3–0.5 using a slow speed Well vertical diamond wire saw. The 250 μm root radius notches were placed to a depth of a/W = 0.3 using a 45° V-notch cutter coated with TiN. Fatigue precracks roughly 500 μm in length were initiated from specimens with a notch root radius of 110 μm, to a depth a/W = 0.5.

The fracture toughness tests were performed according to ASTM E399-90. The specimens were loaded in three-point bending on a 20 Kip MTS servohydraulic machine operated at a constant displacement rate of 0.1 mm/min. Load, load point displacement and, in some specimens, crack opening displacement (COD) were monitored during the test. In the latter case, a clip gage was placed across the crack mouth in order to instantaneously measure the COD. The resulting fracture surfaces were examined in a Hitachi S-4500 field emission SEM operated at 15 keV.

2.3. *Fractography*

The fractured compression and tension specimens were examined both macroscopically and microscopically. The macroscopic fracture plane angle (with respect to the loading axis) was measured by a Bausch & Lomb contour measuring projector for each specimen tested. The fracture surfaces of all specimens were examined using a Hitachi S4500 field emission scanning electron microscope (SEM) and a Leica Wild M8 zoom stereomicroscope.

3. Results and discussion

3.1. *Flow behavior*

All specimens tested exhibited load vs. displacement traces which were linear to failure. There have been some reports [5,9] of limited plastic flow of bulk metallic glass in compression, although none of the investigations [5,9,14] report such behavior in tension. The tension specimens tested at 1 atm (i.e. 0.1 MPa) exhibited fracture surfaces which were oriented nominally perpendicular to the tensile axis. Multiple fragments were exhibited by such tests and all surfaces were (nominally) macroscopically perpendicular to the tensile axis and well removed from the specimen shoulders. All other specimens (i.e. compression, tension with confining pressure) exhibited fracture surfaces which were clearly oriented at some angle to the tensile axis, as shown in

Fig. 1. Non-propagating microcracks/shear bands parallel to the fracture surface were also observed in those specimens. Fracture again occurred within the gage length and well removed from the loading fixtures in all but one specimen out of a total of 13 specimens tested.

Fig. 2 illustrates the large effects of stress state (i.e. tension, compression, and level of superimposed pressure) on the macroscopic orientation of the fracture surface with respect to the loading axis. The average angle between the macroscopic fracture plane and the loading axis in the compression specimens was $41.6 \pm 2.1°$, while that of the tension specimens tested with superimposed hydrostatic pressure between 50 and 575 MPa was $57.0 \pm 3.7°$. Both values are significantly different from those reported on thin ribbons of amorphous alloys, which exhibited nominally 45° [15–17], while recent tests on bulk metallic glasses tested in tension and compression obtained fracture planes oriented at 53–58° and 44–46°, respectively [9]. The source(s) of such differences in fracture plane angle are under current investigation and may be due to subtle differences in specimen geometry, specimen preparation, alloy chemistry and/or test conditions. Fig. 3 summarizes the relatively minor effect of superimposed pressure on the flow/fracture stress, over the range of conditions tested. The average tensile fracture stress obtained on three specimens tested at 0.1 MPa was 1978 ± 20 MPa, while that obtained in three specimens tested in compression was 1911 ± 64 MPa. The slightly higher scatter in fracture stress exhibited by the compression specimens could in part be due to residual polishing scratches noticed on the surface of the specimen which exhibited the lowest fracture stress. The seven tension tests conducted with confining pressure exhibited a fracture stress of 1910 ± 71 MPa. Neither tension testing with superimposed pressure nor compression testing produced a significant change in the macroscopic fracture strain, which was essentially zero for all of the conditions presently tested. Typical fractographs of specimens tested at different level of superimposed hydrostatic pressure are shown in Fig. 4. The specimens tested at 1 atm exhibited a "feathery" fracture morphology as shown in Fig. 4a. At higher magnification, it was observed that the "feathery" feature consisted of what resembled equiaxed shallow dimples. Fig. 4b shows the typical "vein" pattern observed on the fracture surfaces of the compression specimens and the tension specimens tested under superimposed hydrostatic pressure.

The results of the present work, in which the flow/fracture stress is independent of hydrostatic pressure over the range tested, suggest that the amorphous Zr–Ti–Ni–Cu–Be alloy behaves as a von Mises material. This is in agree-

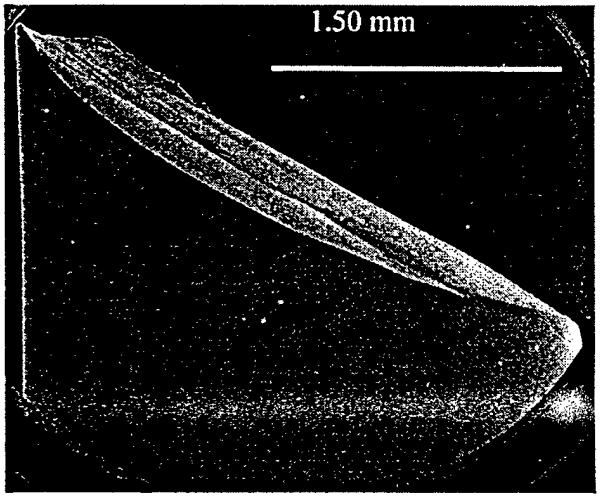

Fig. 1. Typical failure mode of tension specimens tested with superimposed hydrostatic pressure. Compression specimens tested at 1 atm exhibited similar macroscopic features although at a different angle to the loading axis. Tension specimens tested at 1 atm failed in multiple pieces, each of which was macroscopically at 90° to the tensile axis.

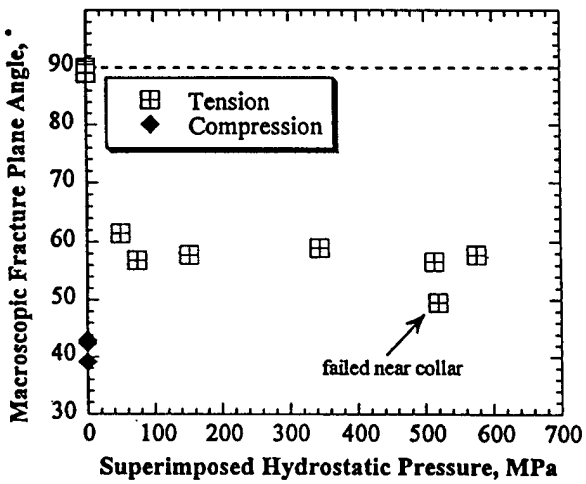

Fig. 2. Macroscopic fracture plane angle as a function of superimposed hydrostatic pressure.

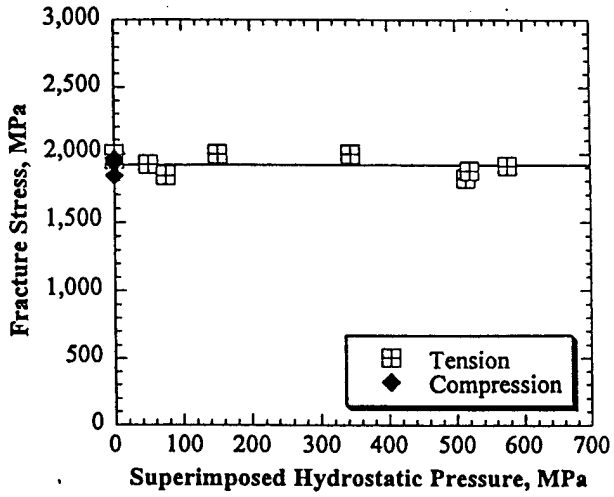

Fig. 3. Fracture stress as a function of superimposed hydrostatic pressure.

ment with the work on a similar bulk metallic glass [5] as well as other work conducted on the earlier metallic glass systems, [18–20] as discussed previously [14]. However, the lack of a pressure dependence to the flow/fracture behavior is somewhat in contrast to various flow models [21–24] of amorphous materials, as discussed elsewhere [14].

A relatively strong normal stress dependence was demonstrated by the deviation of the macroscopic fracture plane from the maximum shear plane (i.e. 45°), as shown in Fig. 2. Such behavior has also been observed in amorphous $Pd_{40}Ni_{40}P_{20}$ [20]. Such results suggest a normal stress dependence to the flow/fracture behavior, in conflict with the apparent lack of pressure dependence to the flow/fracture behavior obtained presently. Although a pressure modified Mohr–Coulomb yield criterion was proposed by Donovan [20] to accommodate a similar observation on an amorphous $Pd_{40}Ni_{40}P_{20}$ alloy, no tests were conducted with superimposed pressure in that work. Experiments over a wider range of stress states are currently underway in order to resolve this apparent internal inconsistency of results.

3.2. Fracture Toughness

All of the fracture toughness tests exhibited essentially linear load vs. load point displacement/COD traces, while the effect(s) of changes in the notch root radius on the fracture toughness for specimens, taken from both 4 and 7 mm thick plate thicknesses, are shown in Fig. 5. The fracture toughness, K_Q, of the bulk metallic glass obtained from seven fatigue precracked specimens

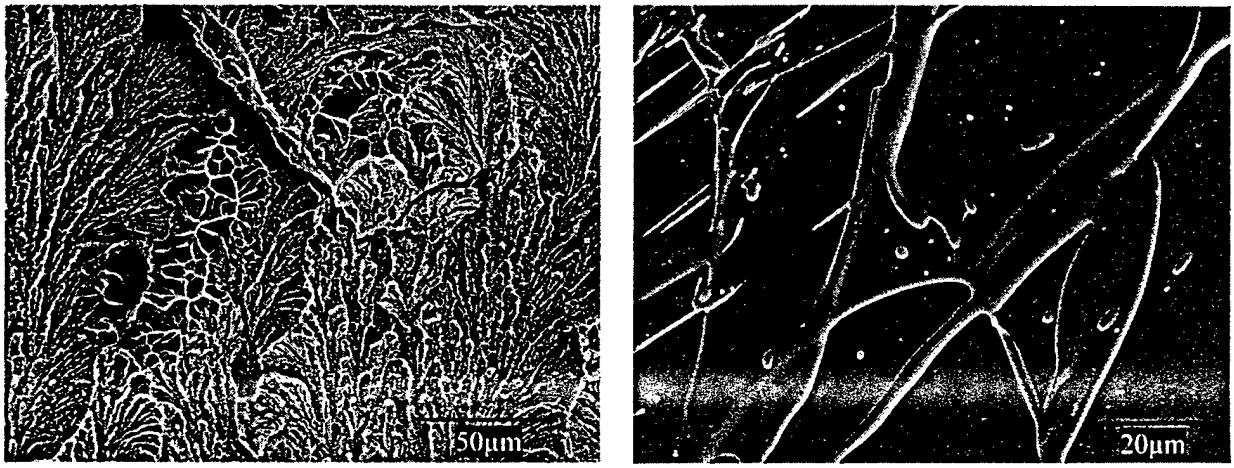

(a) (b)

Fig. 4. Typical fractograph of a tension specimen: (a) tested at 1 atm; (b) tested under superimposed hydrostatic pressure.

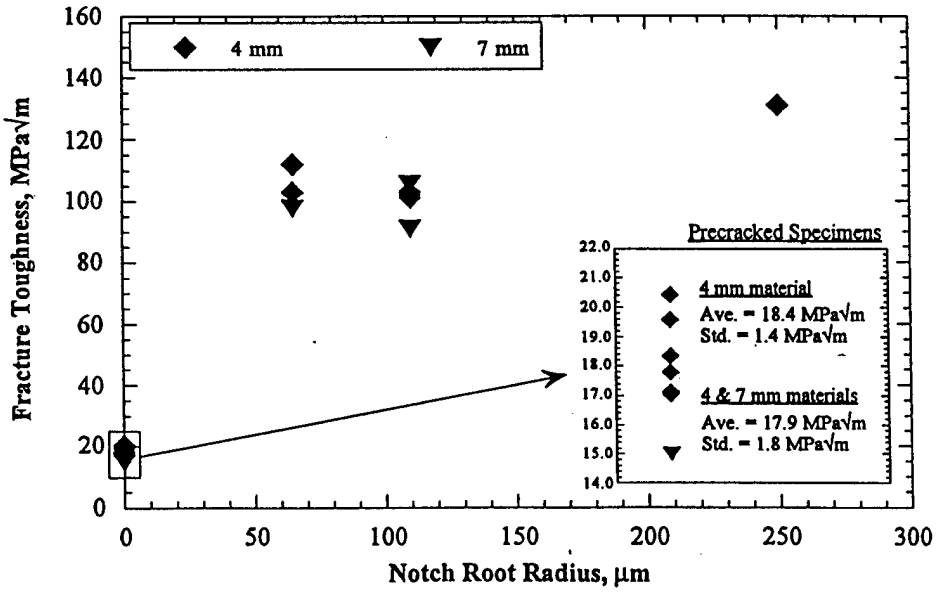

Fig. 5. Fracture toughness as a function of notch root radius.

comprising both plate thicknesses is 17.9 ± 1.8 MPa$\sqrt{m}$. The yield strength obtained from tension specimens tested at 1 atm was 1978 ± 20 MPa, providing a calculated plane-strain plastic zone size of less than 4.3 μm which is well within the thickness requirements for a valid K_{IC} measurement. However, the fracture toughness data obtained on specimens containing fatigue precracks are reported as K_Q instead of K_{IC} because the ΔK levels used during fatigue precracking exceeded those specified by ASTM E399-90 and thus the toughness data obtained on the fatigue precracked specimens do not strictly conform to the K_{IC} standard, as indicated in an earlier paper on the 4 mm plate material [25]. The toughness values reported in Fig. 5 for the notched specimens are similarly reported as K_Q due to the lack of a fatigue precrack. The notched toughness data obtained on specimens taken from both 4 and 7 mm thick plates was essentially identical.

To the authors knowledge, these are the first reported fracture toughness values obtained on fatigue precracked bend specimens taken from both 4 and 7 mm plates of the bulk amorphous alloy. There have been other recent reports [7, 9,12] on the toughness of similar, but not identical materials and specimen geometries. The notch bend toughness obtained on both thinner (i.e. 2.2 mm thick) [12] and thicker (i.e. 5 mm thick) [9] material was reported as 57.2 ± 2.3 MPa$\sqrt{m}$ [12] and 51–56 MPa$\sqrt{m}$ [9], while the fracture toughness reported on somewhat thicker (i.e. 7 mm thick) fatigue precracked compact tension specimens was 55.0 ± 5.0 MPa$\sqrt{m}$ [7]. The present results obtained on the fatigue precracked bend specimens are significantly lower than these previous reports [7,9,12] for the toughness and are significantly lower than the notched toughness values shown in Fig. 5. The apparent discrepancy between the

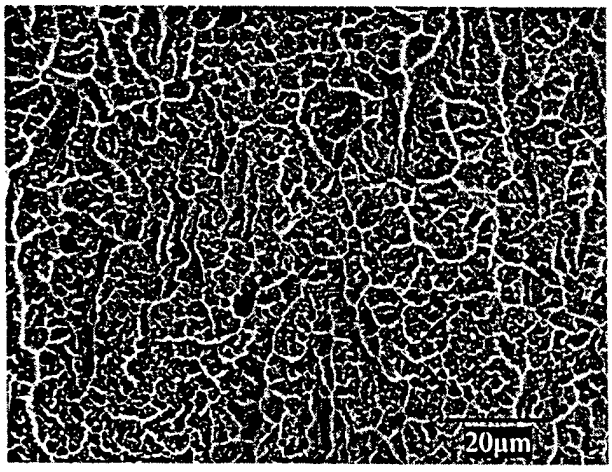

Fig. 6. Typical fractograph of a fatigue precracked specimen in the overload region.

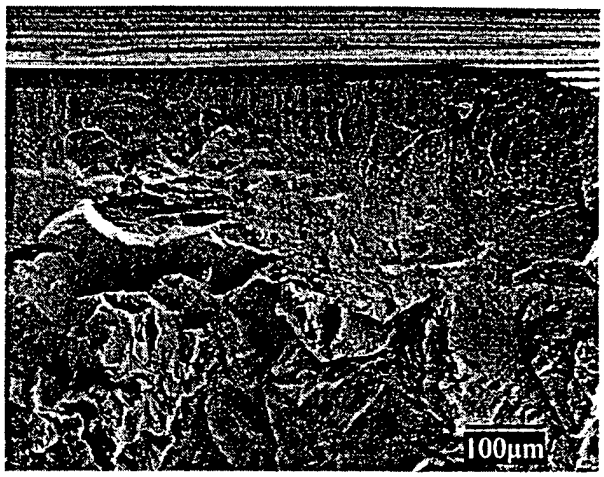

(a)

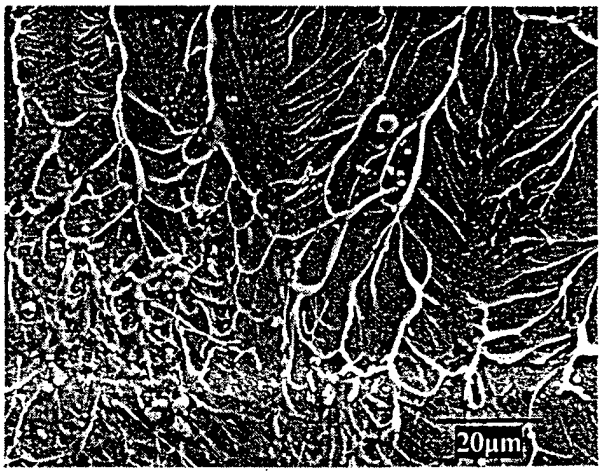

(b)

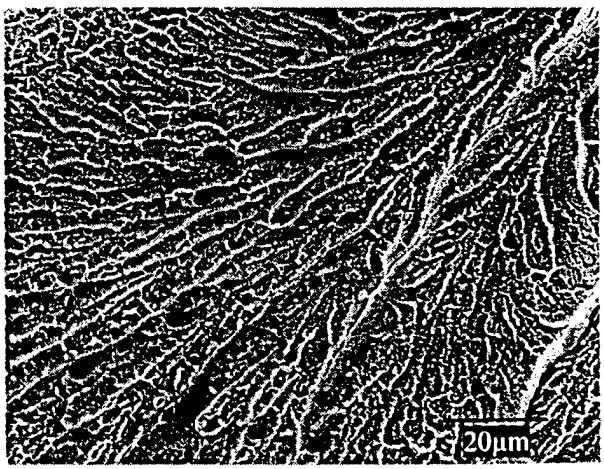

(c)

Fig. 7. Typical fractograph of a notched specimen: (a) notch region (notch at the top of photograph); (b) planar region below the notch; (c) overload region.

fatigue precracked toughness values presently reported and one of the former reports [12] has been discussed previously [25] as in part due to the use of a relatively blunt notch and thinner specimen (i.e. 2.2 mm) instead of the fatigue precracked thicker (i.e. 4 or 7 mm) specimens presently reported. The crack path profile observed presently was also significantly affected by the notch root radius. The fatigue precracked specimens exhibited a very planar crack front while the notched specimens exhibited extensive shear banding at the notch as well as significant crack bifurcation once the crack propagated. Both processes (i.e. multiple shear banding, crack bifurcation) should absorb more energy than the planar fracture mode exhibited by the fatigue precracked specimens, consistent with the relative differences in the measured toughness reported in Fig. 5 on going from the fatigue precracked specimens to those containing somewhat blunter notches. The stress concentration and the stress state ahead of a fatigue precrack is also more severe than that obtained ahead of a blunter notch. Earlier work on the notched toughness [12] of a similar bulk metallic glass also reported such crack bifurcation in a notched specimen, although fatigue precracked specimens were not tested in that work. It is not presently clear if the difference in fracture toughness is due to specimen geometry effects, slight compositional differences, differences in the fatigue precracking procedures, or a combination of these factors. Separate investigations are currently underway in each of these areas.

Figs. 6 and 7 present SEM fractographs of the fatigue precracked bend specimens and notched toughness bend specimens, respectively. The overload region of the fatigue precracked specimen, shown in Fig. 6, was analyzed via stereo SEM images and revealed what appeared to be shallow dimples similar to "feathery" features observed in the tension specimens tested at 1 atm. The notched toughness specimens also exhibited two different types of features as shown in Fig. 7a. Very near the notch root (i.e. planar region), the fracture surface exhibited features suggestive of local melting and/or viscous flow, as revealed by the globular features and "spattered" appearance of the fracture surface in Fig. 7b. The overload region, Fig. 7c, exhibited the "feathery" fracture morphology, as observed in tension specimens tested at 1 atm.

Acknowledgements

The authors gratefully acknowledge the supply of material by Dr. A. Peker and Dr. M. Tenhover of Amorphous Technologies International, Inc. (ATI) and helpful interactions with Dr. W.L. Johnson (Keck Laboratory of Engineering Materials, California Institute of Technology). Discussions with Professor A. Argon and Professor F. Spaepen are also gratefully acknowledged. The project is under financial support of AFOSR-AASERT F49420- 96-1-0228 and Howmet Corporation.

References

[1] Peker A, Johnson WL. Applied Physics Letters 1993;63:2342.
[2] Inoue A, Zhang T, Masumoto T. Mater Trans Japan Inst Metals 1990;31:425.
[3] Zhang T, Inoue A, Masumoto T. Mater Trans Japan Inst Metals 1991;32:1005.
[4] Inoue A, Nakamura Y, Nishiyama N, Masumoto T. Mater Trans Japan Inst Metals 1992;33:937.
[5] Bruck HA, Christman T, Rosakis AJ, Johnson WL. Scripta metall 1994;30:429.
[6] Bruck HA, Rosakis AJ, Johnson WL. J Mater Res 1996;11(2):503.
[7] Gilbert CJ, Ritchie RO, Johnson WL. Applied Physics Letters 1997;71:476.
[8] Gilbert CJ, Lippmann JM, Ritchie RO. Scripta mater 1998;38(4):537.
[9] Liu CT, et al. Metall Mater Trans 1998;29A:1811.
[10] Schroeder V, Gilbert CJ, Ritchie RO. Scripta mater 1998;38(10):1481.
[11] Schroeder V, Gilbert CJ, Ritchie RO. Scripta mater 1999;40(9):1057.
[12] Conner RD, Rosakis AJ, Johnson WL, Owen DM. Scripta mater 1997;37(9):1373.
[13] Lewandowski JJ, Lowhaphandu P. Inter Mater Rev 1998;43(4):145.
[14] Lowhaphandu P, Montgomery SL, Lewandowski JJ. Scripta mater 1999;41(1):19.
[15] Davis LA, Kavesh S. J Mater Sci 1975;10:453.
[16] Leamy HJ, Chen HS, Wang TT. Metall Trans 1972;3:699.
[17] Pampillo CA, Polk DE. Acta metall 1974;22:741.
[18] Kimura H, Masumoto T. Acta metall 1980;28:1663.
[19] Kimura H, Masumoto T. Acta metall 1980;28:1677.
[20] Donovan PE. Acta metall 1989;37:445.
[21] Spaepen F. Acta metall 1977;25:407.
[22] Argon AS. Acta metall 1979;27:47.
[23] Argon AS, Shi LT. Acta metall 1983;31:499.
[24] Steif PS. J Mech Phys Solids 1983;31:359.
[25] Lowhaphandu P, Lewandowski JJ. Scripta mater 1998;38(12):1811.